Advanced courses in Macroscopic Physical Chemistry
(Han-sur-Lesse winterschool 2005)

THEORY OF POLYMER DYNAMICS

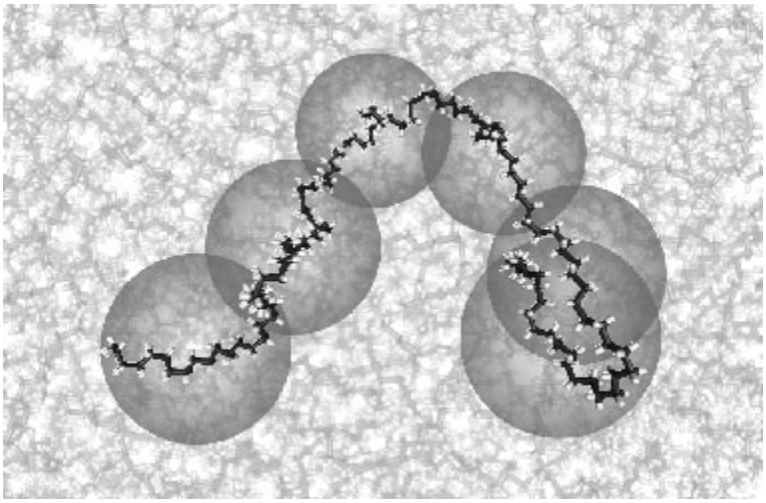

Johan T. Padding

Theoretical Chemistry
University of Cambridge
United Kingdom

UNIVERSITY OF CAMBRIDGE

Contents

Preface

These lecture notes provide a concise introduction to the theory of polymer dynamics. The reader is assumed to have a reasonable math background (including some knowledge of probability and statistics, partial differential equations, and complex functions) and have some knowledge of statistical mechanics.

We will first introduce the concept of a Gaussian chain (chapter 1), which is a simple bead and spring model representing the *equilibrium* properties of a polymer. By adding friction and random forces to such a chain, one arrives at a description of the *dynamics* of a single polymer. For simplicity we will first neglect any hydrodynamic interactions (HIs). Surprisingly, this so-called Rouse model (chapter 2) is a very good approximation for low molecular weight polymers at high concentrations.

The next two chapters deal with extensions of the Rouse model. In chapter 3 we will treat HIs in an approximate way and arrive at the Zimm model, appropriate for dilute polymers. In chapter 4 we will introduce the tube model, in which the primary result of entanglements in high molecular weight polymers is the constraining of a test chain to longitudinal motion along its own contour.

The following books have been very helpful in the preparation of these lectures:

- W.J. Briels, *Theory of Polymer Dynamics*, Lecture Notes, Uppsala (1994). Also available on *http://www.tn.utwente.nl/cdr/PolymeerDictaat/*.
- M. Doi and S.F. Edwards, *The Theory of Polymer Dynamics* (Clarendon, Oxford, 1986).
- D.M. McQuarrie, *Statistical Mechanics* (Harper & Row, New York, 1976).

I would especially like to thank Prof. Wim Briels, who introduced me to the subject of polymer dynamics. His work formed the basis of a large part of these lecture notes.

Johan Padding, Cambridge, January 2005.

Chapter 1

The Gaussian chain

1.1 Similarity of global properties

Polymers are long linear macromolecules made up of a large number of chemical units or monomers, which are linked together through covalent bonds. The number of monomers per polymer may vary from a hundred to many thousands. We can describe the conformation of a polymer by giving the positions of its backbone atoms. The positions of the remaining atoms then usually follow by simple chemical rules. So, suppose we have $N+1$ monomers, with $N+1$ position vectors

$$\mathbf{R}_0, \mathbf{R}_1, \ldots, \mathbf{R}_N.$$

We then have N bond vectors

$$\mathbf{r}_1 = \mathbf{R}_1 - \mathbf{R}_0, \ldots, \mathbf{r}_N = \mathbf{R}_N - \mathbf{R}_{N-1}.$$

Much of the static and dynamic behavior of polymers can be explained by models which are surprisingly simple. This is possible because the global, large scale properties of polymers do not depend on the chemical details of the monomers, except for some species-dependent "effective" parameters. For example, one can measure the end-to-end vector, defined as

$$\mathbf{R} = \mathbf{R}_N - \mathbf{R}_0 = \sum_{i=1}^{N} \mathbf{r}_i. \tag{1.1}$$

If the end-to-end vector is measured for a large number of polymers in a melt, one will find that the distribution of end-to-end vectors is Gaussian and that the root mean squared end-to-end distance scales with the square root of the number of bonds, $\sqrt{\langle R^2 \rangle} \propto \sqrt{N}$, irrespective of the chemical details. This is a consequence of the central limit theorem.

1.2 The central limit theorem

Consider a chain consisting of N independent bond vectors $\mathbf{r}_i$. By this we mean that the orientation and length of each bond is independent of all others. A justification will be given at the end of this section. The probability density in configuration space $\Psi\left(\mathbf{r}^N\right)$ may then be written as

$$\Psi\left(\mathbf{r}^N\right) = \prod_{i=1}^{N} \psi(\mathbf{r}_i)\,. \tag{1.2}$$

Assume further that the bond vector probability density $\psi(\mathbf{r}_i)$ depends only on the length of the bond vector and has zero mean, $\langle \mathbf{r}_i \rangle = \mathbf{0}$. For the second moment we write

$$\left\langle r^2 \right\rangle = \int \mathrm{d}^3 r\; r^2 \psi(r) \equiv b^2, \tag{1.3}$$

where we have defined the statistical segment (or Kuhn) length b,. Let $\Omega(\mathbf{R};N)$ be the probability distribution function for the end-to-end vector given that we have a chain of N bonds,

$$\Omega(\mathbf{R};N) = \left\langle \delta\left(\mathbf{R} - \sum_{i=1}^{N} \mathbf{r}_i\right)\right\rangle, \tag{1.4}$$

where δ is the Dirac-delta function. The central limit theorem then states that

$$\Omega(\mathbf{R};N) = \left\{\frac{3}{2\pi N b^2}\right\}^{3/2} \exp\left\{-\frac{3R^2}{2Nb^2}\right\}, \tag{1.5}$$

i.e., that the end-to-end vector has a Gaussian distribution with zero mean and a variance given by

$$\left\langle R^2 \right\rangle = Nb^2. \tag{1.6}$$

In order to prove Eq. (1.5) we write

$$\begin{aligned}
\Omega(\mathbf{R};N) &= \frac{1}{(2\pi)^3}\int \mathrm{d}\mathbf{k}\, \left\langle \exp\left\{\mathrm{i}\mathbf{k}\cdot\left(\mathbf{R} - \sum_i \mathbf{r}_i\right)\right\}\right\rangle \\
&= \frac{1}{(2\pi)^3}\int \mathrm{d}\mathbf{k}\, \mathrm{e}^{\mathrm{i}\mathbf{k}\cdot\mathbf{R}} \left\langle \exp\left\{-\mathrm{i}\mathbf{k}\cdot\sum_i \mathbf{r}_i\right\}\right\rangle \\
&= \frac{1}{(2\pi)^3}\int \mathrm{d}\mathbf{k}\, \mathrm{e}^{\mathrm{i}\mathbf{k}\cdot\mathbf{R}} \left\{\int \mathrm{d}\mathbf{r}\, \mathrm{e}^{-\mathrm{i}\mathbf{k}\cdot\mathbf{r}} \psi(\mathbf{r})\right\}^N .
\end{aligned} \tag{1.7}$$

For $\mathbf{k} = \mathbf{0}$, the Fourier transform of $\psi(\mathbf{r})$ will be equal to one. Because $\psi(\mathbf{r})$ has zero mean and finite second moment, the Fourier transform of $\psi(\mathbf{r})$ will have its maximum around $\mathbf{k} = \mathbf{0}$ and go to zero for large values of $\mathbf{k}$. Raising such a function to the N'th power leaves us with a function that differs from zero only very close to the origin, and which may be approximated by

$$\begin{aligned}\left\{\int \mathrm{d}\mathbf{r}\, \mathrm{e}^{-\mathrm{i}\mathbf{k}\cdot\mathbf{r}}\psi(\mathbf{r})\right\}^N &\approx \left\{1-\frac{1}{2}\left\langle(\mathbf{k}\cdot\mathbf{r})^2\right\rangle\right\}^N \\ &\approx 1-\frac{1}{2}N\left\langle(\mathbf{k}\cdot\mathbf{r})^2\right\rangle \\ &= 1-\frac{1}{6}Nk^2b^2 \end{aligned} \tag{1.8}$$

for small values of $\mathbf{k}$, and by zero for the values of $\mathbf{k}$ where $1-\frac{1}{6}Nk^2b^2$ is negative. This again may be approximated by $\exp\left\{-\frac{1}{6}Nk^2b^2\right\}$ for all values of $\mathbf{k}$. Then

$$\begin{aligned}\Omega(\mathbf{R};N) &= \frac{1}{(2\pi)^3}\int \mathrm{d}\mathbf{k}\, \exp\left\{\mathrm{i}\mathbf{k}\cdot\mathbf{R}-\frac{1}{6}Nk^2b^2\right\} \\ &= I(R_x)\,I(R_y)\,I(R_z) \end{aligned} \tag{1.9}$$

$$\begin{aligned} I(R_x) &= \frac{1}{2\pi}\int \mathrm{d}k_x\, \exp\left\{\mathrm{i}R_xk_x-\frac{1}{6}Nb^2k_x^2\right\} \\ &= \left\{\frac{3}{2\pi Nb^2}\right\}^{1/2}\exp\left\{-\frac{3R_x^2}{2Nb^2}\right\}. \end{aligned} \tag{1.10}$$

Combining Eqs. (1.9) and (1.10) we get Eq. (1.5).

Using $\Omega(\mathbf{R};N)$, we can obtain an interesting insight in the thermodynamic behaviour of a polymer chain. The entropy of a chain in which the end-to-end vector $\mathbf{R}$ is kept fixed, absorbing all constants into a reference entropy, is given by

$$S(\mathbf{R};N) = k_B \ln\Omega(\mathbf{R};N) = S_0 - \frac{3kR^2}{2Nb^2}, \tag{1.11}$$

where k_B is Boltzmann's constant. The free energy is then

$$A = U - TS = A_0 + \frac{3k_BTR^2}{2Nb^2}, \tag{1.12}$$

where T is the temperature. We see that the free energy is related quadratically to the end-to-end distance, as if the chain is a harmonic (Hookean) spring with spring constant $3k_BT/Nb^2$. Unlike an ordinary spring, however, the strength of the spring *increases* with temperature! These springs are often referred to as entropic springs.

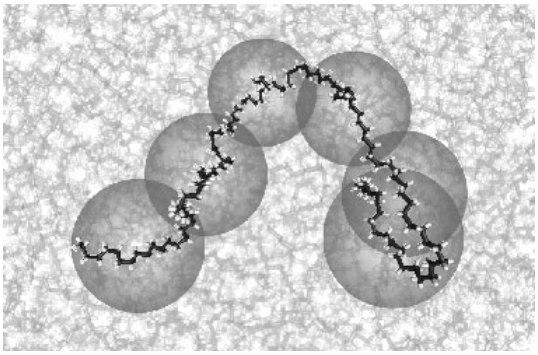

Figure 1.1: A polyethylene chain represented by segments of $\lambda = 20$ monomers. If enough consecutive monomers are combined into one segment, the vectors connecting these segments become independent of each other.

Of course, in a real polymer the vectors connecting consecutive monomers do not take up random orientations. However, if enough (say λ) consecutive monomers are combined into one segment with center-of-mass position $\mathbf{R}_i$, the vectors connecting the segments ($\mathbf{R}_i - \mathbf{R}_{i-1}$, $\mathbf{R}_{i+1} - \mathbf{R}_i$, etcetera) become independent of each other,[1] see Fig. 1.1. If the number of segments is large enough, the end-to-end vector distribution, according to the central limit theorem, will be Gaussianly distributed and the local structure of the polymer appears only through the statistical segment length b.

1.3 The Gaussian chain

Now we have established that global conformational properties of polymers are largely independent of the chemical details, we can start from the simplest model available, consistent with a Gaussian end-to-end distribution. This model is one in which every bond vector itself is Gaussian distributed,

$$\psi(\mathbf{r}) = \left\{ \frac{3}{2\pi b^2} \right\}^{3/2} \exp\left\{ -\frac{3}{2b^2} r^2 \right\}. \tag{1.13}$$

[1] We assume we can ignore long range excluded volume interactions. This is not always the case. Consider building the chain by consecutively adding monomers. At every step there are on average more monomers in the back than in front of the last monomer. Therefore, in a good solvent, the chain can gain entropy by going out, and being larger than a chain in which the new monomer does not feel its predecessors. In a bad solvent two monomers may feel an effective attraction at short distances. In case this attraction is strong enough it may cause the chain to shrink. Of course there is a whole range between good and bad, and at some point both effects cancel and Eq. (1.5) holds true. A solvent having this property is called a Θ-solvent. In a polymer melt, every monomer is isotropically surrounded by other monomers, and there is no way to decide whether the surrounding monomers belong to the same chain as the monomer at hand or to a different one. Consequently there will be no preferred direction and the polymer melt will act as a Θ-solvent. Here we shal restrict ourselves to such melts and Θ-solvents.

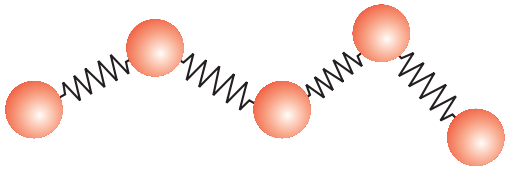

Figure 1.2: The gaussian chain can be represented by a collection of beads connected by harmonic springs of strength $3k_BT/b^2$.

Such a Gaussian chain is often represented by a mechanical model of beads connected by harmonic springs, as in Fig. 1.2. The potential energy of such a chain is given by:

$$\Phi(\mathbf{r}_1,\ldots,\mathbf{r}_N) = \frac{1}{2}k\sum_{i=1}^{N} r_i^2. \tag{1.14}$$

It is easy to see that if the spring constant k is chosen equal to

$$k = \frac{3k_BT}{b^2}, \tag{1.15}$$

the Boltzmann distribution of the bond vectors obeys Eqs. (1.2) and (1.13). The Gaussian chain is used as a starting point for the Rouse model.

Problems

1-1. A way to test the Gaussian character of a distribution is to calculate the ratio of the fourth and the square of the second moment. Show that if the end-to-end vector has a Gaussian distribution then

$$\frac{\langle R^4\rangle}{\langle R^2\rangle^2} = 5/3.$$

Chapter 2

The Rouse model

2.1 From statics to dynamics

In the previous chapter we have introduced the Gaussian chain as a model for the equilibrium (static) properties of polymers. We will now adjust it such that we can use it to calculate dynamical properties as well. A prerequisite is that the polymer chains are not very long, otherwise entanglements with surrounding chains will highly constrain the molecular motions.

When a polymer chain moves through a solvent every bead, whether it represents a monomer or a larger part of the chain, will continuously collide with the solvent molecules. Besides a systematic friction force, the bead will experience random forces, resulting in Brownian motion. In the next sections we will analyze the equations associated with Brownian motion, first for the case of a single bead, then for the Gaussian chain. Of course the motion of a bead through the solvent will induce a velocity field in the solvent which will be felt by all the other beads. To first order we might however neglect this effect and consider the solvent as being some kind of indifferent ether, only producing the friction. When applied to dilute polymeric solutions, this model gives rather bad results, indicating the importance of hydrodynamic interactions. When applied to polymeric melts the model is much more appropriate, because in polymeric melts the friction may be thought of as being caused by the motion of a chain relative to the rest of the material, which to a first approximation may be taken to be at rest; propagation of a velocity field like in a normal liquid is highly improbable, meaning there is no hydrodynamic interaction.

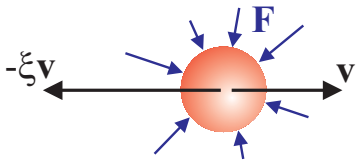

Figure 2.1: A spherical bead moving with velocity $\mathbf{v}$ will experience a friction force $-\xi\mathbf{v}$ opposite to its velocity and random forces $\mathbf{F}$ due to the continuous bombardment of solvent molecules.

2.2 Friction and random forces

Consider a spherical bead of radius a and mass m moving in a solvent. Because on average the bead will collide more often on the front side than on the back side, it will experience a systematic force proportional with its velocity, and directed opposite to its velocity. The bead will also experience a random or stochastic force $\mathbf{F}(t)$. These forces are summarized in Fig. 2.1 The equations of motion then read[1]

$$\frac{\mathrm{d}\mathbf{r}}{\mathrm{d}t} = \mathbf{v} \tag{2.1}$$

$$\frac{\mathrm{d}\mathbf{v}}{\mathrm{d}t} = -\xi\mathbf{v}+\mathbf{F}. \tag{2.2}$$

In Appendix A we show that the friction constant ξ is given by

$$\xi = \zeta/m = 6\pi\eta_s a/m, \tag{2.3}$$

where η_s is the viscosity of the solvent.

Solving Eq. (2.2) yields

$$\mathbf{v}(t) = \mathbf{v}_0 \mathrm{e}^{-\xi t} + \int_0^t \mathrm{d}\tau\, \mathrm{e}^{-\xi(t-\tau)}\mathbf{F}(t). \tag{2.4}$$

where $\mathbf{v}_0$ is the initial velocity. We will now determine averages over all possible realizations of $\mathbf{F}(t)$, with the initial velocity as a condition. To this end we have to make some assumptions about the stochastic force. In view of its chaotic character, the following assumptions seem to be appropriate for its *average* properties:

$$\langle \mathbf{F}(t) \rangle = \mathbf{0} \tag{2.5}$$

$$\langle \mathbf{F}(t) \cdot \mathbf{F}(t') \rangle_{\mathbf{v}_0} = C_{\mathbf{v}_0}\delta(t-t') \tag{2.6}$$

[1]Note that we have divided all forces by the mass m of the bead. Consequently, $\mathbf{F}(t)$ is an acceleration and the friction constant ξ is a frequency.

where $C_{\mathbf{v}_0}$ may depend on the initial velocity. Using Eqs. (2.4) - (2.6), we find

$$\begin{aligned}
\langle \mathbf{v}(t) \rangle_{\mathbf{v}_0} &= \mathbf{v}_0 \mathrm{e}^{-\xi t} + \int_0^t \mathrm{d}\tau\, \mathrm{e}^{-\xi(t-\tau)} \langle \mathbf{F}(\tau) \rangle_{\mathbf{v}_0} \\
&= \mathbf{v}_0 \mathrm{e}^{-\xi t} \qquad (2.7) \\
\langle \mathbf{v}(t) \cdot \mathbf{v}(t) \rangle_{\mathbf{v}_0} &= v_0^2 \mathrm{e}^{-2\xi t} + 2 \int_0^t \mathrm{d}\tau\, \mathrm{e}^{-\xi(2t-\tau)} \mathbf{v}_0 \cdot \langle \mathbf{F}(\tau) \rangle_{\mathbf{v}_0} \\
&\quad + \int_0^t \mathrm{d}\tau' \int_0^t \mathrm{d}\tau\, \mathrm{e}^{-\xi(2t-\tau-\tau')} \left\langle \mathbf{F}(\tau) \cdot \mathbf{F}(\tau') \right\rangle_{\mathbf{v}_0} \\
&= v_0^2 \mathrm{e}^{-2\xi t} + \frac{C_{\mathbf{v}_0}}{2\xi} \left(1 - \mathrm{e}^{-2\xi t} \right). \qquad (2.8)
\end{aligned}$$

The bead is in thermal equilibrium with the solvent. According to the equipartition theorem, for large t, Eq. (2.8) should be equal to $3k_BT/m$, from which it follows that

$$\left\langle \mathbf{F}(t) \cdot \mathbf{F}(t') \right\rangle = 6 \frac{k_B T \xi}{m} \delta(t - t'). \qquad (2.9)$$

This is one manifestation of the fluctuation-dissipation theorem, which states that the systematic part of the microscopic force appearing as the friction is actually determined by the correlation of the random force.

Integrating Eq. (2.4) we get

$$\mathbf{r}(t) = \mathbf{r}_0 + \frac{\mathbf{v}_0}{\xi} \left(1 - \mathrm{e}^{-\xi t} \right) + \int_0^t \mathrm{d}\tau \int_0^\tau \mathrm{d}\tau'\, \mathrm{e}^{-\xi(\tau-\tau')} \mathbf{F}(\tau'), \qquad (2.10)$$

from which we calculate the mean square displacement

$$\left\langle (\mathbf{r}(t) - \mathbf{r}_0)^2 \right\rangle_{\mathbf{v}_0} = \frac{v_0^2}{\xi^2} \left(1 - \mathrm{e}^{-\xi t} \right)^2 + \frac{3k_BT}{m\xi^2} \left(2\xi t - 3 + 4\mathrm{e}^{-\xi t} - \mathrm{e}^{-2\xi t} \right). \qquad (2.11)$$

For very large t this becomes

$$\left\langle (\mathbf{r}(t) - \mathbf{r}_0)^2 \right\rangle = \frac{6k_BT}{m\xi} t, \qquad (2.12)$$

from which we get the Einstein equation

$$D = \frac{k_BT}{m\xi} = \frac{k_BT}{\zeta}, \qquad (2.13)$$

where we have used $\left\langle (\mathbf{r}(t) - \mathbf{r}_0)^2 \right\rangle = 6Dt$. Notice that the diffusion coefficient D is independent of the mass m of the bead.

From Eq. (2.7) we see that the bead loses its memory of its initial velocity after a time span $\tau \approx 1/\xi$. Using equipartition its initial velocity may be put equal to $\sqrt{3k_BT/m}$. The distance l it travels, divided by its diameter then is

$$\frac{l}{a} = \frac{\sqrt{3k_BT/m}}{a\xi} = \sqrt{\frac{\rho k_BT}{9\pi\eta_s^2 a}}, \tag{2.14}$$

where ρ is the mass density of the bead. Typical values are $l/a \approx 10^{-2}$ for a nanometre sized bead and $l/a \approx 10^{-4}$ for a micrometre sized bead in water at room temperature. We see that the particles have hardly moved at the time possible velocity gradients have relaxed to equilibrium. When we are interested in timescales on which particle configurations change, we may restrict our attention to the space coordinates, and average over the velocities. The time development of the distribution of particles on these time scales is governed by the Smoluchowski equation.

In Appendix B we shall derive the Smoluchowski equation and show that the explicit equations of motion for the particles, i.e. the Langevin equations, which lead to the Smoluchowski equation are

$$\frac{\mathrm{d}\mathbf{r}}{\mathrm{d}t} = -\frac{1}{\zeta}\nabla\Phi + \nabla D + \mathbf{f} \tag{2.15}$$

$$\langle \mathbf{f}(t) \rangle = \mathbf{0} \tag{2.16}$$

$$\langle \mathbf{f}(t)\mathbf{f}(t') \rangle = 2D\bar{\mathbf{I}}\delta(t-t'). \tag{2.17}$$

where $\bar{\mathbf{I}}$ denotes the 3-dimensional unit matrix $\mathrm{I}_{\alpha\beta} = \delta_{\alpha\beta}$. We use these equations in the next section to derive the equations of motion for a polymer.

2.3 The Rouse chain

Suppose we have a Gaussian chain consisting of $N+1$ beads connected by N springs of strength $k = 3k_BT/b^2$, see section 1.3. If we focus on one bead, while keeping all other beads fixed, we see that the external field Φ in which that bead moves is generated by connections to its predecessor and successor. We assume that each bead feels the same friction ζ, that its motion is overdamped, and that the diffusion coefficient $D = k_BT/\zeta$ is independent of the position $\mathbf{R}_n$ of the bead. This model for a polymer is called the Rouse chain. According to Eqs. (2.15)-

(2.17) the Langevin equations describing the motion of a Rouse chain are

$$\frac{\mathrm{d}\mathbf{R}_0}{\mathrm{d}t} = -\frac{3k_BT}{\zeta b^2}(\mathbf{R}_0-\mathbf{R}_1)+\mathbf{f}_0 \tag{2.18}$$

$$\frac{\mathrm{d}\mathbf{R}_n}{\mathrm{d}t} = -\frac{3k_BT}{\zeta b^2}(2\mathbf{R}_n-\mathbf{R}_{n-1}-\mathbf{R}_{n+1})+\mathbf{f}_n \tag{2.19}$$

$$\frac{\mathrm{d}\mathbf{R}_N}{\mathrm{d}t} = -\frac{3k_BT}{\zeta b^2}(\mathbf{R}_N-\mathbf{R}_{N-1})+\mathbf{f}_N \tag{2.20}$$

$$\langle \mathbf{f}_n(t)\rangle = \mathbf{0} \tag{2.21}$$

$$\left\langle \mathbf{f}_n(t)\mathbf{f}_m\left(t'\right)\right\rangle = 2D\bar{\mathbf{I}}\delta_{nm}\delta(t-t'). \tag{2.22}$$

Eq. (2.19) applies when $n = 1,\ldots,N-1$.

2.4 Normal mode analysis

Equations (2.18) - (2.20) are $(3N+3)$ coupled stochastic differential equations. In order to solve them, we will first ignore the stochastic forces $\mathbf{f}_n$ and try specific solutions of the following form:

$$\mathbf{R}_n(t) = \mathbf{X}(t)\cos(an+c). \tag{2.23}$$

The equations of motion then read

$$\frac{d\mathbf{X}}{dt}\cos c = -\frac{3k_BT}{\zeta b^2}\{\cos c-\cos(a+c)\}\mathbf{X} \tag{2.24}$$

$$\frac{d\mathbf{X}}{dt}\cos(na+c) = -\frac{3k_BT}{\zeta b^2}4\sin^2(a/2)\cos(na+c)\mathbf{X} \tag{2.25}$$

$$\frac{d\mathbf{X}}{dt}\cos(Na+c) = -\frac{3k_BT}{\zeta b^2}\{\cos(Na+c)-\cos((N-1)a+c)\}\mathbf{X}, \tag{2.26}$$

where we have used

$$\begin{aligned}&2\cos(na+c)-\cos((n-1)a+c)-\cos((n+1)a+c)\\ &\quad=\cos(na+c)\{2-2\cos a\}=\cos(na+c)4\sin^2(a/2).\end{aligned} \tag{2.27}$$

The boundaries of the chain, Eqs. (2.24) and (2.26), are consistent with Eq. (2.25) if we choose

$$\cos c-\cos(a+c) = 4\sin^2(a/2)\cos c \tag{2.28}$$

$$\cos(Na+c)-\cos((N-1)a+c) = 4\sin^2(a/2)\cos(Na+c), \tag{2.29}$$

which is equivalent to

$$\cos(a-c) = \cos c \tag{2.30}$$
$$\cos\left((N+1)a+c\right) = \cos(Na+c). \tag{2.31}$$

We find independent solutions from

$$a-c = c \tag{2.32}$$
$$(N+1)a+c = p2\pi - Na - c, \tag{2.33}$$

where p is an integer. So finally

$$a = \frac{p\pi}{N+1},\ c = a/2 = \frac{p\pi}{2(N+1)}. \tag{2.34}$$

Eq. (2.23), with a and c from Eq. (2.34), decouples the set of differential equations. To find the general solution to Eqs. (2.18) to (2.22) we form a linear combination of all *independent* solutions, formed by taking p in the range $p = 0,\ldots,N$:

$$\mathbf{R}_n = \mathbf{X}_0 + 2\sum_{p=1}^{N} \mathbf{X}_p \cos\left[\frac{p\pi}{N+1}(n+\frac{1}{2})\right]. \tag{2.35}$$

The factor 2 in front of the summation is only for reasons of convenience. Making use of[2]

$$\frac{1}{N+1}\sum_{n=0}^{N} \cos\left[\frac{p\pi}{N+1}(n+\frac{1}{2})\right] = \delta_{p0} \qquad (0 \le p < 2(N+1)), \tag{2.36}$$

we may invert this to

$$\mathbf{X}_p = \frac{1}{N+1}\sum_{n=0}^{N} \mathbf{R}_n \cos\left[\frac{p\pi}{N+1}(n+\frac{1}{2})\right]. \tag{2.37}$$

The equations of motion then read

$$\frac{\mathrm{d}\mathbf{X}_p}{\mathrm{d}t} = -\frac{3k_BT}{\zeta b^2} 4\sin^2\left(\frac{p\pi}{2(N+1)}\right)\mathbf{X}_p + \mathbf{F}_p \tag{2.38}$$
$$\left\langle \mathbf{F}_p(t)\right\rangle = \mathbf{0} \tag{2.39}$$
$$\left\langle \mathbf{F}_0(t)\mathbf{F}_0(t')\right\rangle = \frac{2D}{N+1}\bar{\mathbf{I}}\delta(t-t') \tag{2.40}$$
$$\left\langle \mathbf{F}_p(t)\mathbf{F}_q(t')\right\rangle = \frac{D}{N+1}\bar{\mathbf{I}}\delta_{pq}\delta(t-t') \qquad (p+q>0) \tag{2.41}$$

[2]The validity of Eq. (2.36) is evident when $p = 0$ or $p = N+1$. In the remaining cases the sum may be evaluated using $\cos(na+c) = 1/2(\mathrm{e}^{ina}\mathrm{e}^{ic} + \mathrm{e}^{-ina}\mathrm{e}^{-ic})$. The result then is

$$\frac{1}{N+1}\sum_{n=0}^{N} \cos\left[\frac{p\pi}{N+1}(n+\frac{1}{2})\right] = \frac{1}{2(N+1)}\frac{\sin(p\pi)}{\sin\left(\frac{p\pi}{2(N+1)}\right)},$$

which is consistent with Eq. (2.36).

where $p,q = 0,\ldots,N$. $\mathbf{F}_p$ is a weighted average of the stochastic forces $\mathbf{f}_n$,

$$\mathbf{F}_p = \frac{1}{N+1}\sum_{n=0}^{N}\mathbf{f}_n \cos\left[\frac{p\pi}{N+1}(n+\frac{1}{2})\right], \tag{2.42}$$

and is therefore itself a stochastic variable, characterised by its first and second moments, Eqs. (2.39) - (2.41).

2.5 Rouse mode relaxation times and amplitudes

Eqs. (2.38) - (2.41) form a decoupled set of $3(N+1)$ stochastic differential equations, each of which describes the fluctuations and relaxations of a normal mode (a Rouse mode) of the Rouse chain. It is easy to see that the zeroth Rouse mode, $\mathbf{X}_0$, is the position of the centre-of-mass $\mathbf{R}_G = \sum_n \mathbf{R}_n/(N+1)$ of the polymer chain. The mean square displacement of the centre-of-mass, $g_{\rm cm}(t)$ can easily be calculated:

$$\mathbf{X}_0(t) = \mathbf{X}_0(0) + \int_0^t \mathrm{d}\tau\, \mathbf{F}_0(\tau) \tag{2.43}$$

$$\begin{aligned} g_{\rm cm}(t) &= \left\langle (\mathbf{X}_0(t)-\mathbf{X}_0(0))^2 \right\rangle = \left\langle \int_0^t \mathrm{d}\tau \int_0^t \mathrm{d}\tau'\, \mathbf{F}_0(\tau)\cdot\mathbf{F}_0(\tau') \right\rangle \\ &= \frac{6D}{N+1}t \equiv 6D_G t. \end{aligned} \tag{2.44}$$

So the diffusion coefficient of the centre-of-mass of the polymer is given by $D_G = D/(N+1) = k_BT/[(N+1)\zeta]$. Notice that the diffusion coefficient scales inversely proportional to the length (and weight) of the polymer chain. All other modes $1 \le p \le N$ describe independent vibrations of the chain leaving the centre-of-mass unchanged; Eq. (2.37) shows that Rouse mode $\mathbf{X}_p$ descibes vibrations of a wavelength corresponding to a subchain of N/p segments. In the applications ahead of us, we will frequently need the time correlation functions of these Rouse modes. From Eq. (2.38) we get

$$\mathbf{X}_p(t) = \mathbf{X}_p(0)\mathrm{e}^{-t/\tau_p} + \int_0^t \mathrm{d}\tau\, \mathrm{e}^{-(t-\tau)/\tau_p}\mathbf{F}_p(\tau), \tag{2.45}$$

where the characteristic relaxation time τ_p is given by

$$\tau_p = \frac{\zeta b^2}{3k_BT}\left[4\sin^2\left(\frac{p\pi}{2(N+1)}\right)\right]^{-1} \approx \frac{\zeta b^2(N+1)^2}{3\pi^2 k_BT}\frac{1}{p^2}. \tag{2.46}$$

The last approximation is valid for large wavelengths, in which case $p \ll N$. Multiplying Eq. (2.45) by $\mathbf{X}_p(0)$ and taking the average over all possible realisations

of the random force, we find

$$\left\langle \mathbf{X}_p(t)\cdot\mathbf{X}_p(0)\right\rangle = \left\langle X_p^2\right\rangle \exp\left(-t/\tau_p\right). \tag{2.47}$$

From these equations it is clear that the lower Rouse modes, which represent motions with larger wavelengths, are also slower modes. The relaxation time of the slowest mode, $p=1$, is often referred to as the Rouse time τ_R.

We now calculate the equilibrium expectation values of X_p^2, i.e., the amplitudes of the normal modes. To this end, first consider the statistical weight of a configuration $\mathbf{R}_0,\ldots,\mathbf{R}_N$ in Carthesian coordinates,

$$P\left(\mathbf{R}_0,\ldots,\mathbf{R}_N\right) = \frac{1}{Z}\exp\left[-\frac{3}{2b^2}\sum_{n=1}^{N}\left(\mathbf{R}_n-\mathbf{R}_{n-1}\right)^2\right], \tag{2.48}$$

where Z is a normalization constant (the partition function). We can use Eq. (2.35) to find the statistical weight of a configuration in Rouse coordinates. Since the transformation to the Rouse coordinates is a linear transformation from one set of orthogonal coordinates to another, the corresponding Jacobian is simply a constant. The statistical weight therefore reads

$$P\left(\mathbf{X}_0,\ldots,\mathbf{X}_N\right) = \frac{1}{Z}\exp\left[-\frac{12}{b^2}(N+1)\sum_{p=1}^{N}\mathbf{X}_p\cdot\mathbf{X}_p\sin^2\left(\frac{p\pi}{2(N+1)}\right)\right]. \tag{2.49}$$

[Exercise: show this] Since this is a simple product of independent Gaussians, the amplitudes of the Rouse modes can easily be calculated:

$$\left\langle X_p^2\right\rangle = \frac{b^2}{8(N+1)\sin^2\left(\frac{p\pi}{2(N+1)}\right)} \approx \frac{(N+1)b^2}{2\pi^2}\frac{1}{p^2}. \tag{2.50}$$

Again, the last approximation is valid when $p \ll N$. Using the amplitudes and relaxation times of the Rouse modes, Eqs. (2.50) and (2.46) respectively, we can now calculate all kinds of dynamic quantities of the Rouse chain.

2.6 Correlation of the end-to-end vector

The first dynamic quantity we are interested in is the time correlation function of the end-to-end vector $\mathbf{R}$. Notice that

$$\mathbf{R} = \mathbf{R}_N - \mathbf{R}_0 = 2\sum_{p=1}^{N}\mathbf{X}_p\left\{(-1)^p-1\right\}\cos\left[\frac{p\pi}{2(N+1)}\right]. \tag{2.51}$$

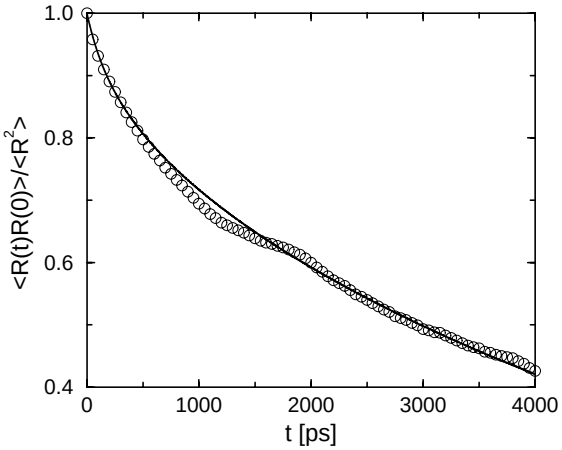

Figure 2.2: Molecular dynamics simulation results for the orientational correlation function of the end-to-end vector of a $C_{120}H_{242}$ polyethylene chain under melt conditions (symbols), compared with the Rouse model prediction (solid line). J.T. Padding and W.J. Briels, J. Chem. Phys. **114**, 8685 (2001).

Because the Rouse mode amplitudes decay as p^{-2}, our results will be dominated by p values which are extremely small compared to N. We therefore write

$$\mathbf{R} = -4\sum_{p=1}^{N}{}' \mathbf{X}_p, \tag{2.52}$$

where the prime at the summation sign indicates that only terms with odd p should occur in the sum. Then

$$\begin{aligned} \langle \mathbf{R}(t)\cdot\mathbf{R}(0)\rangle &= 16\sum_{p=1}^{N}{}' \langle \mathbf{X}_p(t)\cdot\mathbf{X}_p(0)\rangle \\ &= \frac{8b^2}{\pi^2}(N+1)\sum_{p=1}^{N}{}' \frac{1}{p^2}\mathrm{e}^{-t/\tau_p}. \end{aligned} \tag{2.53}$$

The characteristic decay time at large t is τ_1, which is proportional to $(N+1)^2$.

Figure 2.2 shows that Eq. (2.53) gives a good description of the time correlation function of the end-to-end vector of a real polymer chain in a melt (provided the polymer is not much longer than the entanglement length).

2.7 Segmental motion

In this section we will calculate the mean square displacements $g_{\mathrm{seg}}(t)$ of the individual segments. Using Eq. (2.35) and the fact that different modes are not correlated, we get for segment n

$$\begin{aligned} \left\langle (\mathbf{R}_n(t)-\mathbf{R}_n(0))^2 \right\rangle &= \left\langle (\mathbf{X}_0(t)-\mathbf{X}_0(0))^2 \right\rangle \\ &+4\sum_{p=1}^{N} \left\langle (\mathbf{X}_p(t)-\mathbf{X}_p(0))^2 \right\rangle \cos^2\left[\frac{p\pi}{N+1}(n+\frac{1}{2})\right]. \end{aligned} \tag{2.54}$$

Averaging over all segments, and introducing Eqs. (2.44) and (2.47), the mean square displacement of a typical segment in the Rouse model is

$$\begin{aligned} g_{\rm seg}(t) &= \frac{1}{N+1}\sum_{n=0}^{N}\left\langle (\mathbf{R}_n(t)-\mathbf{R}_n(0))^2\right\rangle \\ &= 6D_G t + 4\sum_{p=1}^{N}\left\langle X_p^2\right\rangle\left(1-{\rm e}^{-t/\tau_p}\right). \end{aligned} \tag{2.55}$$

Two limits may be distinguished. First, when t is very large, $t \gg \tau_1$, the first term in Eq. (2.55) will dominate, yielding

$$g_{\rm seg}(t) \approx 6D_G t \qquad (t \gg \tau_1). \tag{2.56}$$

This is consistent with the fact that the polymer as a whole diffuses with diffusion coefficient D_G.

Secondly, when $t \ll \tau_1$ the sum over p in Eq. (2.55) dominates. If $N \gg 1$ the relaxation times can be approximated by the right hand side of Eq. (2.46), the Rouse mode amplitudes can be approximated by the right hand side of Eq. (2.50), and the sum can be replaced by an integral,

$$\begin{aligned} g_{\rm seg}(t) &= \frac{2b^2}{\pi^2}(N+1)\int_0^\infty {\rm d}p\,\frac{1}{p^2}\left(1-{\rm e}^{-tp^2/\tau_1}\right) \\ &= \frac{2b^2}{\pi^2}(N+1)\int_0^\infty {\rm d}p\,\frac{1}{\tau_1}\int_0^t {\rm d}t'\,{\rm e}^{-t'p^2/\tau_1} \\ &= \frac{2b^2}{\pi^2}\frac{(N+1)}{\tau_1}\frac{1}{2}\sqrt{\pi\tau_1}\int_0^t {\rm d}t'\,\frac{1}{\sqrt{t'}} \\ &= \left(\frac{12k_BTb^2}{\pi\zeta}\right)^{1/2} t^{1/2} \qquad (\tau_N \ll t \ll \tau_1, N \gg 1). \end{aligned} \tag{2.57}$$

So, at short times the mean square displacement of a typical segment is subdiffusive with an exponent 1/2, and is independent of the number of segments N in the chain.

Figure 2.3 shows the mean square displacement of monomers (circles) and centre-of-mass (squares) of an unentangled polyethylene chain in its melt. Observe that the chain motion is in agreement with the Rouse model prediction, but only for displacements larger than the square statistical segment length b^2.

2.8 Stress and viscosity

We will now calculate the viscosity of a solution or melt of Rouse chains. To this end we will first introduce the macroscopic concepts of stress and shear flow.

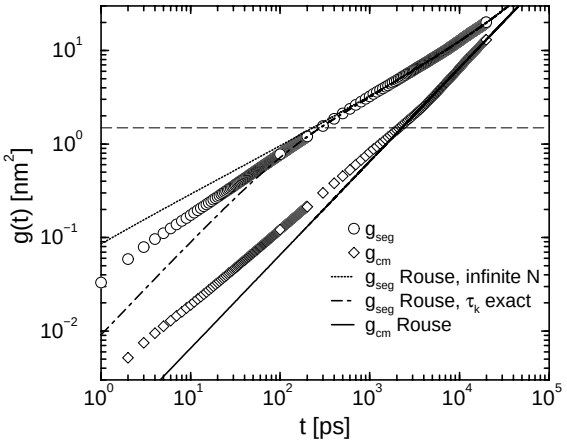

Figure 2.3: Molecular dynamics simulation results for the mean square displacements of a $C_{120}H_{242}$ polyethylene chain under melt conditions (symbols). The dotted and dot-dashed lines are Rouse predictions for a chain with an infinite number of modes and for a finite Rouse chain, respectively. The horizontal line is the statistical segment length b^2. J.T. Padding and W.J. Briels, J. Chem. Phys. **114**, 8685 (2001).

Then we will show how the viscosity can be calculated from a microscopic model such as the Rouse model.

2.8.1 The stress tensor

Suppose the fluid velocity on a macroscopic scale is described by the fluid velocity field $\mathbf{v}(\mathbf{r})$. When two neighbouring fluid volume elements move with different velocities, they will experience a friction force proportional to the area of the surface between the two fluid volume elements. Moreover, even without relative motion, the volume elements will be able to exchange momentum through the motions of, and interactions between, the constituent particles.

All the above forces can conveniently be summarized in the stress tensor. Consider a surface element of size dA and normal $\hat{\mathbf{t}}$. Let d$\mathbf{F}$ be the force exerted by the fluid below the surface element on the fluid above the fluid element. Then we define the stress tensor $\bar{\mathbf{S}}$ by

$$\mathrm{d}F_\alpha = -\sum_\beta S_{\alpha\beta}\hat{t}_\beta \mathrm{d}A = -\left(\bar{\mathbf{S}}\cdot\hat{\mathbf{t}}\right)_\alpha \mathrm{d}A, \tag{2.58}$$

where α and β run from 1 to 3 (or x, y, and z). It is easy to show that the total force $\mathbf{F}$ on a volume element V is given by

$$\mathbf{F} = V\boldsymbol{\nabla}\cdot\bar{\mathbf{S}}. \tag{2.59}$$

In the case of simple fluids the stress tensor consists of one part which is independent of the fluid velocity, and a viscous part which depends linearly on the *instantaneous* derivatives $\partial v_\alpha/\partial r_\beta$. In Appendix A we elaborate on this, and calculate the velocity field and friction on a sphere moving in a simple liquid. In the

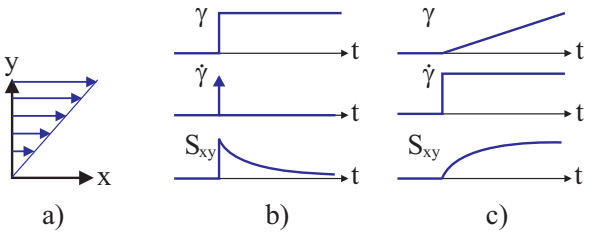

Figure 2.4: Shear flow in the xy-plane (a). Strain γ, shear rate $\dot{\gamma}$, and stress S_{xy} versus time t for sudden shear strain (b) and sudden shear flow (c).

more general case of complex fluids, the stress tensor depends on the *history* of fluid flow (the fluid has a memory) and has both viscous and elastic components.

2.8.2 Shear flow and viscosity

Shear flows, for which the velocity components are given by

$$v_\alpha(\mathbf{r},t) = \sum_\beta \kappa_{\alpha\beta}(t)\, r_\beta, \tag{2.60}$$

are commonly used for studying the viscoelastic properties of complex fluids. If the shear rates $\kappa_{\alpha\beta}(t)$ are small enough, the stress tensor depends linearly on $\bar{\boldsymbol{\kappa}}(t)$ and can be written as

$$S_{\alpha\beta}(t) = \int_{-\infty}^{t} \mathrm{d}\tau\, G(t-\tau)\, \kappa_{\alpha\beta}(\tau), \tag{2.61}$$

where $G(t)$ is called the shear relaxation modulus. $G(t)$ contains the shear stress memory of the complex fluid. This becomes apparent when we consider two special cases, depicted in Fig. 2.4:

(*i*) *Sudden shear strain*. At $t = 0$ a shear strain γ is suddenly applied to a relaxed system. The velocity field is given by

$$v_x(t) = \delta(t)\gamma r_y \tag{2.62}$$
$$v_y(t) = 0 \tag{2.63}$$
$$v_z(t) = 0 \tag{2.64}$$

The stress tensor component of interest is S_{xy}, which now reads

$$S_{xy}(t) = \gamma G(t). \tag{2.65}$$

So $G(t)$ is simply the stress relaxation after a sudden shear strain.

(*ii*) *Sudden shear flow*. At $t = 0$ a shear flow is suddenly switched on:

$$v_x(t) = \Theta(t)\dot{\gamma} r_y \tag{2.66}$$
$$v_y(t) = 0 \tag{2.67}$$
$$v_z(t) = 0 \tag{2.68}$$

Here $\Theta(t)$ is the Heaviside function and $\dot{\gamma}$ is the shear rate. Now S_{xy} is given by

$$S_{xy}(t) = \dot{\gamma} \int_0^t \mathrm{d}\tau \, G(t-\tau), \tag{2.69}$$

In the case of simple fluids, the shear stress is the product of shear rate and the shear viscosity, a characteristic transport property of the fluid (see Appendix A, Eq. (A.3)). Similarly, in the case of complex fluids, the shear viscosity is defined as the ratio of steady-state shear stress and shear rate,

$$\eta = \lim_{t\to\infty} \frac{S_{xy}(t)}{\dot{\gamma}} = \lim_{t\to\infty} \int_0^t \mathrm{d}\tau \, G(t-\tau) = \int_0^\infty \mathrm{d}\tau \, G(\tau). \tag{2.70}$$

The limit $t \to \infty$ must be taken because during the early stages elastic stresses are built up. This expression shows that the integral over the shear relaxation modulus yields the (low shear rate) viscosity.

2.8.3 Microscopic expression for the viscosity and stress tensor

Eq. (2.70) is not very useful as it stands because the viscosity is not related to the microscopic properties of the molecular model. Microscopic expresions for transport properties such as the viscosity can be found by relating the relaxation of a macroscopic disturbance to spontaneous fluctuations in an equilibrium system. Close to equilibrium there is no way to distinguish between spontaneous fluctuations and deviations from equilibrium that are externally prepared. Since one cannot distinguish, according to the regression hypothesis of Onsager, the regression of spontaneous fluctuations should coincide with the relaxation of macroscopic variables to equilibrium. A derivation for the viscosity and many other transport properties can be found in Statistical Mechanics text books. The result for the viscosity is

$$\eta = \frac{V}{k_B T} \int_0^\infty \mathrm{d}\tau \, \left\langle \sigma_{xy}^{\mathrm{micr}}(\tau) \, \sigma_{xy}^{\mathrm{micr}}(0) \right\rangle, \tag{2.71}$$

where V is the volume in which the microscopic stress tensor $\bar{\boldsymbol{\sigma}}^{\mathrm{micr}}$ is calculated. Eq. (2.71) is sometimes referred to as the Green-Kubo expression for the viscosity. Using Onsager's regression hypothesis, it is possible to relate also the integrand of Eq. (2.71) to the shear relaxation modulus $G(t)$ in the macroscopic world:

$$G(t) = \frac{V}{k_B T} \left\langle \sigma_{xy}^{\mathrm{micr}}(t) \, \sigma_{xy}^{\mathrm{micr}}(0) \right\rangle \tag{2.72}$$

The microscopic stress tensor in Eqs. (2.71) and (2.72) is generally defined as

$$\bar{\boldsymbol{\sigma}}^{\mathrm{micr}} = -\frac{1}{V} \sum_{i=1}^{N_{\mathrm{tot}}} \left[M_i (\mathbf{V}_i - \mathbf{v})(\mathbf{V}_i - \mathbf{v}) + \mathbf{R}_i \mathbf{F}_i \right], \tag{2.73}$$

where M_i is the mass and $\mathbf{V}_i$ the velocity of particle i, and $\mathbf{F}_i$ is the force on particle i. Eqs. (2.71) and (2.72) are ensemble averages under equilibrium conditions. We can therefore set the macroscopic fluid velocity field $\mathbf{v}$ to zero. If furthermore we assume that the interactions between the particles are pairwise additive, we find

$$\bar{\boldsymbol{\sigma}}^{\text{micr}} = -\frac{1}{V}\left(\sum_{i=1}^{N_{\text{tot}}} M_i \mathbf{V}_i \mathbf{V}_i + \sum_{i=1}^{N_{\text{tot}}-1}\sum_{j=i+1}^{N_{\text{tot}}} \left(\mathbf{R}_i - \mathbf{R}_j\right)\mathbf{F}_{ij}\right), \tag{2.74}$$

where $\mathbf{F}_{ij}$ is the force that particle j is exerting on particle i.

The sums in Eqs. (2.73) and (2.74) must be taken over all N_{tot} particles in the system, including the solvent particles. At first sight, it would be a tremendous task to calculate the viscosity analytically. Fortunately, for most polymers there is a large separation of time scales between the stress relaxation due to the solvent and the stress relaxation due to the polymers. In most cases we can therefore treat the solvent contribution to the viscosity, denoted by η_s, separately from the polymer contribution. Moreover, because the velocities of the polymer segments are usually overdamped, the polymer stress is dominated by the interactions between the beads. The first (kinetic) part of Eq. (2.73) or (2.74) may then be neglected.

2.8.4 Calculation for the Rouse model

Even if we can treat separately the solvent contribution, the sum over i in Eq. (2.74) must still be taken over all beads of all chains in the system. This is why in real polymer systems the stress tensor is a collective property. In the Rouse model, however, there is no correlation between the dynamics of one chain and the other, so one may just as well analyze the stress relaxation of a single chain and make an ensemble average over all initial configurations.

Using Eqs. (2.35) and (2.74), the microscopic stress tensor of a Rouse chain in a specific configuration, neglecting also the kinetic contributions, is equal to

$$\begin{aligned}
\bar{\boldsymbol{\sigma}}^{\text{micr}} &= \frac{1}{V}\frac{3k_BT}{b^2}\sum_{n=1}^{N}\left(\mathbf{R}_{n-1}-\mathbf{R}_n\right)\left(\mathbf{R}_{n-1}-\mathbf{R}_n\right) \\
&= \frac{1}{V}\frac{48k_BT}{b^2}\sum_{n=1}^{N}\sum_{p=1}^{N}\sum_{q=1}^{N}\mathbf{X}_p\mathbf{X}_q \sin\left(\frac{p\pi n}{N+1}\right)\sin\left(\frac{p\pi}{2(N+1)}\right)\times \\
&\quad \sin\left(\frac{q\pi n}{N+1}\right)\sin\left(\frac{q\pi}{2(N+1)}\right) \\
&= \frac{1}{V}\frac{24k_BT}{b^2}N\sum_{p=1}^{N}\mathbf{X}_p\mathbf{X}_p\sin^2\left(\frac{p\pi}{2(N+1)}\right).
\end{aligned} \tag{2.75}$$

Combining this with the expression for the equilibrium Rouse mode amplitudes, Eq. (2.50), this can be written more concisely as

$$\bar{\boldsymbol{\sigma}}^{\mathrm{micr}} = \frac{3k_BT}{V}\sum_{p=1}^{N}\frac{\mathbf{X}_p\mathbf{X}_p}{\langle X_p^2\rangle}. \tag{2.76}$$

The correlation of the xy-component of the microscopic stress tensor at $t=0$ with the one at $t=t$ is therefore

$$\sigma_{xy}^{\mathrm{micr}}(t)\sigma_{xy}^{\mathrm{micr}}(0) = \left(\frac{3k_BT}{V}\right)^2\sum_{p=1}^{N}\sum_{q=1}^{N}\frac{X_{px}(t)X_{py}(t)X_{qx}(0)X_{qy}(0)}{\langle X_p^2\rangle\langle X_q^2\rangle}. \tag{2.77}$$

To obtain the shear relaxation modulus, according to Eq. (2.72), the ensemble average must be taken over all possible configurations at $t=0$. Now, since the Rouse modes are Gaussian variables, all the ensemble averages of products of an odd number of X_p's are zero and the ensemble averages of products of an even number of X_p's can be written as a sum of products of averages of only two X_p's. For the even term in Eq. (2.77) we find:

$$\begin{aligned}\langle X_{px}(t)X_{py}(t)X_{qx}(0)X_{qy}(0)\rangle &= \langle X_{px}(t)X_{py}(t)\rangle\langle X_{qx}(0)X_{qy}(0)\rangle \\ &+ \langle X_{px}(t)X_{qy}(0)\rangle\langle X_{py}(t)X_{qx}(0)\rangle \\ &+ \langle X_{px}(t)X_{qx}(0)\rangle\langle X_{py}(t)X_{qy}(0)\rangle.\end{aligned} \tag{2.78}$$

The first four ensemble averages equal zero because, for a Rouse chain in equilibrium, there is no correlation between different cartesian components. The last two ensemble averages are nonzero only when $p=q$, since the Rouse modes are mutually orthogonal. Using the fact that all carthesian components are equivalent, and Eq. (2.47), the shear relaxation modulus (excluding the solvent contribution) of a Rouse chain can be expressed as

$$G(t) = \frac{k_BT}{V}\sum_{p=1}^{N}\left[\frac{\langle\mathbf{X}_k(t)\cdot\mathbf{X}_k(0)\rangle}{\langle X_k^2\rangle}\right]^2 = \frac{ck_BT}{N+1}\sum_{p=1}^{N}\exp\left(-2t/\tau_p\right), \tag{2.79}$$

where $c=N/V$ is the number density of beads.

In concentrated polymer systems and melts, the stress is dominated by the polymer contribution. The shear relaxation modulus calculated above predicts a viscosity, at constant monomer concentration c and segmental friction ζ, proportional to N:

$$\begin{aligned}\eta &= \int_0^\infty \mathrm{d}t\,G(t) \approx \frac{ck_BT}{N+1}\frac{\tau_1}{2}\sum_{p=1}^{N}\frac{1}{p^2} \\ &\approx \frac{ck_BT}{N+1}\frac{\tau_1}{2}\frac{\pi^2}{6} = \frac{c\zeta b^2}{36}(N+1).\end{aligned} \tag{2.80}$$

This has been confirmed for concentrated polymers with low molecular weight.[3] Concentrated polymers of high molecular weight give different results, stressing the importance of entanglements. We will deal with this in Chapter 4.

In dilute polymer solutions, we do not neglect the solvent contribution to the stress. The shear relaxation modulus Eq. (2.79) must be augmented by a very fast decaying term, the integral of which is the solvent viscosity η_s, leading to the following expression for the intrinsic viscosity:

$$[\eta] \equiv \lim_{\rho\to 0} \frac{\eta-\eta_s}{\rho\eta_s} \approx \frac{N_{\rm Av}}{M}\frac{1}{\eta_s}\frac{\zeta b^2}{36}(N+1)^2. \tag{2.81}$$

Here, $\rho = cM/(N_{\rm Av}(N+1))$ is the polymer concentration; M is the mol mass of the polymer, and $N_{\rm Av}$ is Avogadro's number. Eq. (2.81) is at variance with experimental results for dilute polymers, signifying the importance of hydrodynamic interactions. These will be included in the next chapter.

Problems

2-1. Why is it obvious that the expression for the end-to-end vector **R**, Eq. (2.52), should only contain Rouse modes of odd mode number p?
2-2. Show that the shear relaxation modulus $G(t)$ of a Rouse chain at short times decays like $t^{-1/2}$ and is given by

$$G(t) = \frac{ck_BT}{N+1}\sqrt{\frac{\pi\tau_1}{8t}} \qquad (\tau_N \ll t \ll \tau_1).$$

[3] A somewhat stronger N dependence is often observed because the density and, more important, the segmental friction coefficient increase with increasing N.

Appendix A: Friction on a slowly moving sphere

We will calculate the fluid flow field around a moving sphere and the resulting friction. To formulate the basic equations for the fluid we utilize the conservation of mass and momentum. The conservation of mass is expressed by the continuity equation

$$\frac{\mathrm{D}\rho}{\mathrm{D}t} = -\rho \boldsymbol{\nabla} \cdot \mathbf{v}, \tag{A.1}$$

and the conservation of momentum by the Navier-Stokes equation

$$\rho \frac{\mathrm{D}}{\mathrm{D}t}\mathbf{v} = \boldsymbol{\nabla} \cdot \bar{\mathbf{S}}. \tag{A.2}$$

Here $\rho(\mathbf{r},t)$ is the fluid density, $\mathbf{v}(\mathbf{r},t)$ the fluid velocity, $\mathrm{D}/\mathrm{D}t \equiv \mathbf{v}\cdot\boldsymbol{\nabla} + \partial/\partial t$ the total derivative, and $\bar{\mathbf{S}}$ is the stress tensor.

We now have to specify the nature of the stress tensor $\bar{\mathbf{S}}$. For a viscous fluid, friction occurs when the distance between two neighbouring fluid elements changes, i.e. they move relative to each other. Most simple fluids can be described by a stress tensor which consists of a part which is independent of the velocity, and a part which depends linearly on the derivatives $\partial v_\alpha/\partial r_\beta$, i.e., where the friction force is proportional to the *instantaneous* relative velocity of the two fluid elements.[4] The most general form of the stress tensor for such a fluid is

$$S_{\alpha\beta} = \eta_s \left\{ \frac{\partial v_\alpha}{\partial r_\beta} + \frac{\partial v_\beta}{\partial r_\alpha} \right\} - \left\{ P + \left(\frac{2}{3}\eta_s - \kappa \right) \boldsymbol{\nabla}\cdot\mathbf{v} \right\} \delta_{\alpha\beta}, \tag{A.3}$$

where η_s is the shear viscosity, κ the bulk viscosity, which is the resistance of the fluid against compression, and P the pressure.

Many flow fields of interest can be described assuming that the fluid is incompressible, i.e. that the density along the flow is constant. In that case $\boldsymbol{\nabla}\cdot\mathbf{v} = 0$, as follows from Eq. (A.1). Assuming moreover that the velocities are small, and that the second order non-linear term $\mathbf{v}\cdot\boldsymbol{\nabla}\mathbf{v}$ may be neglected, we obtain Stokes

[4] The calculations in this Appendix assume that the solvent is an isotropic, unstructured fluid, with a characteristic stress relaxation time which is much smaller than the time scale of any flow experiment. The stress response of such a so-called Newtonian fluid appears to be *instantaneous*. Newtonian fluids usually consist of small and roughly spherical molecules, e.g., water and light oils. Non-Newtonian fluids, on the other hand, usually consist of large or elongated molecules. Often they are structured, either spontaneously or under the influence of flow. Their characteristic stress relaxation time is experimentally accessible. As a consequence, the stress between two non-Newtonian fluid elements generally depends on the *history* of relative velocities, and contains an elastic part. Examples are polymers and self-assembling surfactants.

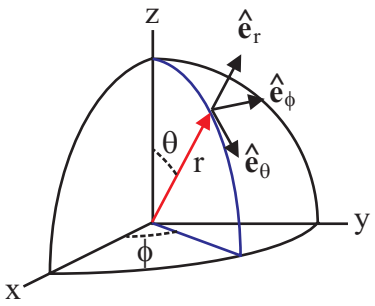

Figure 2.5: Definition of spherical coordinates (r,θ,ϕ) and the unit vectors $\hat{\mathbf{e}}_r$, $\hat{\mathbf{e}}_\theta$, and $\hat{\mathbf{e}}_\phi$.

equation for incompressible flow

$$\rho\frac{\partial \mathbf{v}}{\partial t} = \eta_s\nabla^2\mathbf{v} - \boldsymbol{\nabla}P \tag{A.4}$$

$$\boldsymbol{\nabla}\cdot\mathbf{v} = 0. \tag{A.5}$$

Now consider a sphere of radius a moving with velocity $\mathbf{v}_S$ in a quiescent liquid. Assume that the velocity field is stationary. Referring all coordinates and velocities to a frame which moves with velocity $\mathbf{v}_S$ relative to the fluid transforms the problem into one of a resting sphere in a fluid which, at large distances from the sphere, moves with constant velocity $\mathbf{v}_0 \equiv -\mathbf{v}_S$. The problem is best considered in spherical coordinates (see Fig. 2.5),[5] $\mathbf{v}(\mathbf{r}) = v_r\hat{\mathbf{e}}_r + v_\theta\hat{\mathbf{e}}_\theta + v_\phi\hat{\mathbf{e}}_\phi$, so that $\theta = 0$ in the flow direction. By symmetry the azimuthal component of the fluid velocity is equal to zero, $v_\phi = 0$. The fluid flow at infinity gives the boundary conditions

$$\left.\begin{aligned} v_r &= v_0\cos\theta \\ v_\theta &= -v_0\sin\theta \end{aligned}\right\} \text{ for } r\to\infty. \tag{A.6}$$

Moreover, we will assume that the fluid is at rest on the surface of the sphere (stick boundary conditions):

$$v_r = v_\theta = 0 \text{ for } r = a. \tag{A.7}$$

[5] In spherical coordinates the gradient, Laplacian and divergence are given by

$$\begin{aligned} \boldsymbol{\nabla}f &= \hat{\mathbf{e}}_r\frac{\partial}{\partial r}f + \frac{1}{r}\hat{\mathbf{e}}_\theta\frac{\partial}{\partial\theta}f + \frac{1}{r\sin\theta}\hat{\mathbf{e}}_\phi\frac{\partial}{\partial\phi}f \\ \nabla^2 f &= \frac{1}{r^2}\frac{\partial}{\partial r}\left(r^2\frac{\partial}{\partial r}f\right) + \frac{1}{r^2\sin\theta}\frac{\partial}{\partial\theta}\left(\sin\theta\frac{\partial}{\partial\theta}f\right) + \frac{1}{r^2\sin^2\theta}\frac{\partial^2}{\partial\phi^2}f \\ \boldsymbol{\nabla}\cdot\mathbf{v} &= \frac{1}{r^2}\frac{\partial}{\partial r}\left(r^2 v_r\right) + \frac{1}{r\sin\theta}\frac{\partial}{\partial\theta}\left(\sin\theta v_\theta\right) + \frac{1}{r\sin\theta}\frac{\partial}{\partial\phi}v_\phi. \end{aligned}$$

It can easily be verified that the solution of Eqs. (A.4) - (A.5) is

$$v_r = v_0 \cos\theta \left(1 - \frac{3a}{2r} + \frac{a^3}{2r^3}\right) \tag{A.8}$$

$$v_\theta = -v_0 \sin\theta \left(1 - \frac{3a}{4r} - \frac{a^3}{4r^3}\right) \tag{A.9}$$

$$p - p_0 = -\frac{3}{2}\frac{\eta_s v_0 a}{r^2}\cos\theta. \tag{A.10}$$

We shall now use this flow field to calculate the friction force exerted by the fluid on the sphere. The stress on the surface of the sphere results in the following force per unit area:

$$\begin{aligned} \mathbf{f} &= \bar{\mathbf{S}} \cdot \hat{\mathbf{e}}_r = \hat{\mathbf{e}}_r S_{rr} + \hat{\mathbf{e}}_\theta S_{\theta r} = -\hat{\mathbf{e}}_r \, p|_{(r=a)} + \hat{\mathbf{e}}_\theta \eta_s \left.\frac{\partial v_\theta}{\partial r}\right|_{(r=a)} \\ &= \left(-p_0 + \frac{3\eta_s v_0}{2a}\cos\theta\right)\hat{\mathbf{e}}_r - \frac{3\eta_s v_0}{2a}\sin\theta\hat{\mathbf{e}}_\theta. \end{aligned} \tag{A.11}$$

Integrating over the whole surface of the sphere, only the component in the flow direction survives:

$$F = \int \mathrm{d}\Omega \, a^2 \left[\left(-p_0 + \frac{3\eta_s v_0}{2a}\cos\theta\right)\cos\theta + \frac{3\eta_s v_0}{2a}\sin^2\theta\right] = 6\pi\eta_s a v_0. \tag{A.12}$$

Transforming back to the frame in which the sphere is moving with velocity $\mathbf{v}_S = -\mathbf{v}_0$ through a quiescent liquid, we find for the fluid flow field

$$\mathbf{v}(\mathbf{r}) = \mathbf{v}_S \frac{3a}{4r}\left(1 + \frac{a^2}{3r^2}\right) + \hat{\mathbf{e}}_r \, (\hat{\mathbf{e}}_r \cdot \mathbf{v}_S)\frac{3a}{4r}\left(1 - \frac{a^2}{r^2}\right), \tag{A.13}$$

and the friction on the sphere

$$\mathbf{F} = -\zeta \mathbf{v}_S = -6\pi\eta_s a \mathbf{v}_S. \tag{A.14}$$

F is known as the Stokes friction.

Appendix B: Smoluchowski and Langevin equations

The Smoluchowski equation describes the time evolution of the probability density $\Psi(\mathbf{r},\mathbf{r}_0;t)$ to find a particle at a particular position $\mathbf{r}$ at a particular time t, given it was at $\mathbf{r}_0$ at $t=0$. It is assumed that at every instant of time the particle is in thermal equilibrium with respect to its velocity, i.e., the particle velocity is strongly damped on the Smoluchowski timescale. A flux will exist, given by

$$\mathbf{J}(\mathbf{r},\mathbf{r}_0,t) = -D\boldsymbol{\nabla}\Psi(\mathbf{r},\mathbf{r}_0;t) - \frac{1}{\zeta}\Psi(\mathbf{r},\mathbf{r}_0;t)\boldsymbol{\nabla}\Phi(\mathbf{r}). \tag{B.1}$$

The first term in Eq. (B.1) is the flux due to the diffusive motion of the particle; D is the diffusion coefficient, occurring in $\left\langle(\mathbf{r}(t)-\mathbf{r}_0)^2\right\rangle = 6Dt$. The second term is the flux in the "downhill" gradient direction of the external potential $\Phi(\mathbf{r})$, damped by the friction coefficient ζ. At equilibrium, the flux must be zero and the distribution must be equal to the Boltzmann distribution

$$\Psi_{\mathrm{eq}}(\mathbf{r}) = C\exp\left[-\beta\Phi(\mathbf{r})\right], \tag{B.2}$$

where $\beta = 1/k_BT$ and C a normalization constant. Using this in Eq. (B.1) while setting $\mathbf{J}(\mathbf{r},t)=\mathbf{0}$, leads to the Einstein equation (2.13). In general, we assume that no particles are generated or destroyed, so

$$\frac{\partial}{\partial t}\Psi(\mathbf{r},\mathbf{r}_0;t) = -\boldsymbol{\nabla}\cdot\mathbf{J}(\mathbf{r},\mathbf{r}_0,t). \tag{B.3}$$

Combining Eq. (B.1) with the above equation of particle conservation we arrive at the Smoluchowski equation

$$\frac{\partial}{\partial t}\Psi(\mathbf{r},\mathbf{r}_0;t) = \boldsymbol{\nabla}\cdot\left[\frac{1}{\zeta}\Psi(\mathbf{r},\mathbf{r}_0;t)\boldsymbol{\nabla}\Phi(\mathbf{r})\right] + \boldsymbol{\nabla}\cdot\left[D\boldsymbol{\nabla}\Psi(\mathbf{r},\mathbf{r}_0;t)\right] \tag{B.4}$$

$$\lim_{t\to 0}\Psi(\mathbf{r},\mathbf{r}_0;t) = \delta(\mathbf{r}-\mathbf{r}_0). \tag{B.5}$$

The Smoluchowski equation describes how particle distribution functions change in time and is fundamental to the non-equilibrium statistical mechanics of overdamped particles such as colloids and polymers.

Sometimes it is more advantageous to have explicit equations of motion for the particles instead of distribution functions. Below we shall show that the Langevin equations which lead to the above Smoluchowski equation are:

$$\frac{\mathrm{d}\mathbf{r}}{\mathrm{d}t} = -\frac{1}{\zeta}\boldsymbol{\nabla}\Phi + \boldsymbol{\nabla}D + \mathbf{f} \tag{B.6}$$

$$\langle\mathbf{f}(t)\rangle = \mathbf{0} \tag{B.7}$$

$$\left\langle\mathbf{f}(t)\mathbf{f}(t')\right\rangle = 2D\bar{\mathbf{I}}\delta(t-t'). \tag{B.8}$$

where $\bar{\mathbf{I}}$ denotes the 3-dimensional unit matrix $\mathrm{I}_{\alpha\beta} = \delta_{\alpha\beta}$.

The proof starts with the Chapman-Kolmogorov equation, which in our case reads

$$\Psi(\mathbf{r},\mathbf{r}_0;t+\Delta t) = \int \mathrm{d}\mathbf{r}'\, \Psi(\mathbf{r},\mathbf{r}';\Delta t)\Psi(\mathbf{r}',\mathbf{r}_0;t). \tag{B.9}$$

This equation simply states that the probability of finding a particle at position $\mathbf{r}$ at time $t+\Delta t$, given it was at $\mathbf{r}_0$ at $t=0$, is equal to the probability of finding that particle at position $\mathbf{r}'$ at time t, given it was at position $\mathbf{r}_0$ at time $t=0$, multiplied by the probability that it moved from $\mathbf{r}'$ to $\mathbf{r}$ in the last interval Δt, integrated over all possibilities for $\mathbf{r}'$ (we assume Ψ is properly normalized). In the following we assume that we are always interested in *averages* $\int \mathrm{d}\mathbf{r}\, F(\mathbf{r})\Psi(\mathbf{r},\mathbf{r}_0;t)$ of some function $F(\mathbf{r})$. According to Eq. (B.9) this average at $t+\Delta t$ reads

$$\int \mathrm{d}\mathbf{r}\, F(\mathbf{r})\Psi(\mathbf{r},\mathbf{r}_0;t+\Delta t) = \int \mathrm{d}\mathbf{r} \int \mathrm{d}\mathbf{r}'\, F(\mathbf{r})\Psi(\mathbf{r},\mathbf{r}';\Delta t)\Psi(\mathbf{r}',\mathbf{r}_0;t). \tag{B.10}$$

We shall now perform the integral with respect to $\mathbf{r}$ on the right hand side. Because $\Psi(\mathbf{r},\mathbf{r}';\Delta t)$ differs from zero only when $\mathbf{r}$ is in the neighbourhood of $\mathbf{r}'$, we expand $F(\mathbf{r})$ around $\mathbf{r}'$,

$$F(\mathbf{r}) = F(\mathbf{r}') + \sum_\alpha (r_\alpha - r'_\alpha)\frac{\partial F(\mathbf{r}')}{\partial r'_\alpha} + \frac{1}{2}\sum_{\alpha,\beta}(r_\alpha - r'_\alpha)(r_\beta - r'_\beta)\frac{\partial^2 F(\mathbf{r}')}{\partial r'_\alpha \partial r'_\beta} \tag{B.11}$$

where α and β run from 1 to 3. Introducing this into Eq. (B.10) we get

$$\begin{aligned}
&\int \mathrm{d}\mathbf{r}\, F(\mathbf{r})\Psi(\mathbf{r},\mathbf{r}_0;t+\Delta t) = \\
&\quad \int \mathrm{d}\mathbf{r}' \left\{ \int \mathrm{d}\mathbf{r}\, \Psi(\mathbf{r},\mathbf{r}';\Delta t) \right\} \Psi(\mathbf{r}',\mathbf{r}_0;t)F(\mathbf{r}') + \\
&\quad \sum_\alpha \int \mathrm{d}\mathbf{r}' \left\{ \int \mathrm{d}\mathbf{r}\, (r_\alpha - r'_\alpha)\Psi(\mathbf{r},\mathbf{r}';\Delta t) \right\} \Psi(\mathbf{r}',\mathbf{r}_0;t)\frac{\partial F(\mathbf{r}')}{\partial r'_\alpha} + \\
&\quad \frac{1}{2}\sum_{\alpha,\beta} \int \mathrm{d}\mathbf{r}' \left\{ \int \mathrm{d}\mathbf{r}\, (r_\alpha - r'_\alpha)(r_\beta - r'_\beta)\Psi(\mathbf{r},\mathbf{r}';\Delta t) \right\} \Psi(\mathbf{r}',\mathbf{r}_0;t)\frac{\partial^2 F(\mathbf{r}')}{\partial r'_\alpha \partial r'_\beta}.
\end{aligned} \tag{B.12}$$

Now we evaluate the terms between brackets:

$$\int \mathrm{d}\mathbf{r}\, \Psi(\mathbf{r},\mathbf{r}';\Delta t) = 1 \tag{B.13}$$

$$\int \mathrm{d}\mathbf{r}\, (r_\alpha - r'_\alpha)\Psi(\mathbf{r},\mathbf{r}';\Delta t) = -\frac{1}{\zeta}\frac{\partial \Phi}{\partial r'_\alpha}\Delta t + \frac{\partial D}{\partial r'_\alpha}\Delta t \tag{B.14}$$

$$\int \mathrm{d}\mathbf{r}\, (r_\alpha - r'_\alpha)(r_\beta - r'_\beta)\Psi(\mathbf{r},\mathbf{r}';\Delta t) = 2D\delta_{\alpha\beta}\Delta t, \tag{B.15}$$

which hold true up to first order in Δt. The first equation is obvious. The last two easily follow from the Langevin equations (B.6) - (B.8). Introducing this into Eq. (B.12), dividing by Δt and taking the limit $\Delta t \to 0$, we get

$$\int \mathrm{d}\mathbf{r}\, F(\mathbf{r}) \frac{\partial}{\partial t} \Psi(\mathbf{r}, \mathbf{r}_0; t) = \sum_\alpha \int \mathrm{d}\mathbf{r}' \left\{ \left[-\frac{1}{\zeta} \frac{\partial \Phi}{\partial r'_\alpha} + \frac{\partial D}{\partial r'_\alpha} \right] \frac{\partial F(\mathbf{r}')}{\partial r'_\alpha} + D \frac{\partial^2 F(\mathbf{r}')}{\partial r'^2_\alpha} \right\} \Psi(\mathbf{r}', \mathbf{r}_0; t) \qquad \text{(B.16)}$$

Next we change the integration variable $\mathbf{r}'$ into $\mathbf{r}$ and perform some partial integrations. Making use of $\lim_{|\mathrm{r}|\to\infty} \Psi(\mathbf{r}, \mathbf{r}_0; t) = 0$ and $\nabla^2 (D\Psi) = \boldsymbol{\nabla} \cdot (\Psi \boldsymbol{\nabla} D) + \boldsymbol{\nabla} \cdot (D \boldsymbol{\nabla} \Psi)$, we finally obtain

$$\begin{aligned} &\int \mathrm{d}\mathbf{r}\, F(\mathbf{r}) \frac{\partial}{\partial t} \Psi(\mathbf{r}, \mathbf{r}_0; t) \\ &= \sum_\alpha \int \mathrm{d}\mathbf{r}\, F(\mathbf{r}) \frac{\partial}{\partial r_\alpha} \left[\frac{1}{\zeta} \Psi(\mathbf{r}, \mathbf{r}_0; t) \frac{\partial \Phi}{\partial r_\alpha} \right] + \\ &\quad \sum_\alpha \int \mathrm{d}\mathbf{r}\, F(\mathbf{r}) \left\{ \frac{\partial}{\partial r_\alpha} \left[-\Psi(\mathbf{r}, \mathbf{r}_0; t) \frac{\partial D}{\partial r_\alpha} \right] + \frac{\partial^2}{\partial r_\alpha^2} \left[D \Psi(\mathbf{r}, \mathbf{r}_0; t) \right] \right\} \\ &= \int \mathrm{d}\mathbf{r}\, F(\mathbf{r}) \left\{ \boldsymbol{\nabla} \cdot \left[\frac{1}{\zeta} \Psi(\mathbf{r}, \mathbf{r}_0; t) \boldsymbol{\nabla} \Phi(\mathbf{r}) \right] + \boldsymbol{\nabla} \cdot \left[D \boldsymbol{\nabla} \Psi(\mathbf{r}, \mathbf{r}_0; t) \right] \right\}. \end{aligned} \qquad \text{(B.17)}$$

Because this has to hold true for all possible $F(\mathbf{r})$ we conclude that the Smoluchowski equation (B.4) follows from the Langevin equations (B.6) - (B.8).

Chapter 3

The Zimm model

3.1 Hydrodynamic interactions in a Gaussian chain

In the previous chapter we have focused on the Rouse chain, which gives a good description of the dynamics of unentangled *concentrated* polymer solutions and melts. We will now add hydrodynamic interactions between the beads of a Gaussian chain. This so-called Zimm chain, gives a good description of the dynamics of unentangled *dilute* polymer solutions.

The equations describing hydrodynamic interactions between beads, up to lowest order in the bead separations, are given by

$$\mathbf{v}_i = -\sum_{j=0}^{N} \bar{\boldsymbol{\mu}}_{ij} \cdot \mathbf{F}_j \tag{3.1}$$

$$\bar{\boldsymbol{\mu}}_{ii} = \frac{1}{6\pi\eta_s a}\bar{\mathbf{I}}, \qquad \bar{\boldsymbol{\mu}}_{ij} = \frac{1}{8\pi\eta_s R_{ij}}\left(\bar{\mathbf{I}} + \hat{\mathbf{R}}_{ij}\hat{\mathbf{R}}_{ij}\right). \tag{3.2}$$

Here $\mathbf{v}_i$ is the velocity of bead i, $\mathbf{F}_j$ the force exerted by the fluid on bead j, η_s the solvent viscosity, a the radius of a bead, and $\hat{\mathbf{R}}_{ij} = \mathbf{R}_{ij}/R_{ij}$, where $\mathbf{R}_{ij} = \mathbf{R}_i - \mathbf{R}_j$ is the vector from the position of bead j to the position of bead i. A derivation can be found in Appendix A of this chapter.

In Eq. (3.1), the mobility tensors $\bar{\boldsymbol{\mu}}$ relate the bead velocities to the hydrodynamic forces acting on the beads. Of course there are also conservative forces $-\boldsymbol{\nabla}_k\Phi$ acting on the beads because they are connected by springs. On the Smoluchowski time scale, we assume that the conservative forces make the beads move with constant velocities $\mathbf{v}_k$. This amounts to saying that the forces $-\boldsymbol{\nabla}_k\Phi$ are exactly balanced by the hydrodynamic forces acting on the beads k. In Appendix B we describe the Smoluchowski equation for the beads in a Zimm chain. The

Langevin equations corresponding to this Smoluchowski equation are

$$\frac{\mathrm{d}\mathbf{R}_j}{\mathrm{d}t} = -\sum_k \bar{\boldsymbol{\mu}}_{jk}\cdot\boldsymbol{\nabla}_k\Phi + k_BT\sum_k \boldsymbol{\nabla}_k\cdot\bar{\boldsymbol{\mu}}_{jk} + \mathbf{f}_j \tag{3.3}$$

$$\langle \mathbf{f}_j(t)\rangle = \mathbf{0} \tag{3.4}$$

$$\langle \mathbf{f}_j(t)\mathbf{f}_k(t')\rangle = 2k_BT\bar{\boldsymbol{\mu}}_{jk}\delta(t-t'). \tag{3.5}$$

The reader can easily check that these reduce to the equations of motion of the Rouse chain when hydrodynamic interactions are neglected.

The particular form of the mobility tensor Eq. (3.2) (the Oseen tensor) has the fortunate property

$$\sum_k \boldsymbol{\nabla}_k\cdot\bar{\boldsymbol{\mu}}_{jk} = \mathbf{0}, \tag{3.6}$$

which greatly simplifies Eq. (3.3).

3.2 Normal modes and Zimm relaxation times

If we introduce the mobility tensors Eq. (3.2) into the Langevin equations (3.3) - (3.5), we are left with a completely intractable set of equations. One way out of this is by noting that in equilibrium, on average, the mobility tensor will be proportional to the unit tensor. A simple calculation yields

$$\begin{aligned}\langle\bar{\boldsymbol{\mu}}_{jk}\rangle_{\mathrm{eq}} &= \frac{1}{8\pi\eta_s}\left\langle\frac{1}{R_{jk}}\right\rangle_{\mathrm{eq}}\left(\bar{\mathbf{I}}+\langle\hat{\mathbf{R}}_{jk}\hat{\mathbf{R}}_{jk}\rangle_{\mathrm{eq}}\right)\\ &= \frac{1}{6\pi\eta_s}\left\langle\frac{1}{R_{jk}}\right\rangle_{\mathrm{eq}}\bar{\mathbf{I}}\\ &= \frac{1}{6\pi\eta_s b}\left(\frac{6}{\pi|j-k|}\right)^{\frac{1}{2}}\bar{\mathbf{I}}\end{aligned} \tag{3.7}$$

The next step is to write down the equations of motion of the Rouse modes, using Eqs. (2.35) and (2.37):

$$\frac{\mathrm{d}\mathbf{X}_p}{\mathrm{d}t} = -\sum_{q=1}^{N}\mu_{pq}\frac{3k_BT}{b^2}4\sin^2\left(\frac{q\pi}{2(N+1)}\right)\mathbf{X}_q + \mathbf{F}_p \tag{3.8}$$

$$\langle\mathbf{F}_p(t)\rangle = \mathbf{0} \tag{3.9}$$

$$\langle\mathbf{F}_p(t)\mathbf{F}_q(t')\rangle = k_BT\frac{\mu_{pq}}{N+1}\bar{\mathbf{I}}\delta(t-t'), \tag{3.10}$$

where

$$\mu_{pq} = \frac{2}{N+1}\sum_{j=0}^{N}\sum_{k=0}^{N}\frac{1}{6\pi\eta_s b}\left(\frac{6}{\pi|j-k|}\right)^{\frac{1}{2}}\cos\left[\frac{p\pi}{N+1}(j+\frac{1}{2})\right]\cos\left[\frac{q\pi}{N+1}(k+\frac{1}{2})\right]. \tag{3.11}$$

Eq. (3.8) is still not tractable. It turns out however (see Appendix C for a proof) that for large N approximately

$$\mu_{pq} = \left(\frac{N+1}{3\pi^3 p}\right)^{\frac{1}{2}}\frac{1}{\eta_s b}\delta_{pq}. \tag{3.12}$$

Introducing this result in Eq. (3.8), we see that the Rouse modes, just like with the Rouse chain, constitute a set of decoupled coordinates of the Zimm chain:

$$\frac{d\mathbf{X}_p}{dt} = -\frac{1}{\tau_p}\mathbf{X}_p + \mathbf{F}_p \tag{3.13}$$

$$\langle \mathbf{F}_p(t)\rangle = \mathbf{0} \tag{3.14}$$

$$\langle \mathbf{F}_p(t)\mathbf{F}_q(t')\rangle = k_B T\frac{\mu_{pp}}{N+1}\bar{\mathbf{I}}\delta_{pq}\delta(t-t'), \tag{3.15}$$

where the first term on the right hand side of Eq. (3.13) equals zero when $p = 0$, and otherwise, for $p \ll N$,

$$\tau_p \approx \frac{3\pi\eta_s b^3}{k_B T}\left(\frac{N+1}{3\pi p}\right)^{\frac{3}{2}}. \tag{3.16}$$

Eqs. (3.13) - (3.15) lead to the same exponential decay of the normal mode autocorrelations as in the case of the Rouse chain,

$$\langle \mathbf{X}_p(t)\cdot\mathbf{X}_p(0)\rangle = \langle X_p^2\rangle \exp(-t/\tau_p), \tag{3.17}$$

but with a different distribution of relaxation times τ_p. Notably, the relaxation time of the slowest mode, $p = 1$, scales as $N^{\frac{3}{2}}$ instead of N^2. The amplitudes of the normal modes, however, are the same as in the case of the Rouse chain,

$$\langle X_p^2\rangle \approx \frac{(N+1)b^2}{2\pi^2}\frac{1}{p^2}. \tag{3.18}$$

This is because both the Rouse and Zimm chains are based on the same static model (the Gaussian chain), and only differ in the details of the friction, i.e. they only differ in their kinetics.

3.3 Dynamic properties of a Zimm chain

The diffusion coefficient of (the centre-of-mass of) a Zimm chain can easily be calculated from Eqs. (3.13) - (3.15). The result is

$$\begin{aligned} D_G &= \frac{k_BT}{2}\frac{\mu_{00}}{N+1} = \frac{k_BT}{6\pi\eta_s b}\sqrt{\frac{6}{\pi}}\frac{1}{(N+1)^2}\sum_{j=0}^{N}\sum_{k=0}^{N}\frac{1}{|j-k|^{\frac{1}{2}}} \\ &\approx \frac{k_BT}{6\pi\eta_s b}\sqrt{\frac{6}{\pi}}\frac{1}{N^2}\int_0^N \mathrm{d}j\int_0^N \mathrm{d}k\,\frac{1}{|j-k|^{\frac{1}{2}}} = \frac{8}{3}\frac{k_BT}{6\pi\eta_s b}\sqrt{\frac{6}{\pi N}}. \end{aligned} \tag{3.19}$$

The diffusion coefficient now scales with $N^{-1/2}$, in agreement with experiments on dilute polymer solutions.

The similarities between the Zimm chain and the Rouse chain enable us to quickly calculate various other dynamic properties. For example, the time correlation function of the end-to-end vector is given by Eq. (2.53), but now with the relaxation times τ_p given by Eq. (3.16). Similarly, the segmental motion can be found from Eq. (2.55), and the shear relaxation modulus (excluding the solvent contribution) from Eq. (2.79). Hence, for dilute polymer solutions, the Zimm model predicts an intrinsic viscosity given by

$$[\eta] = \frac{\eta-\eta_s}{\rho\eta_s} = \frac{N_{\mathrm{Av}}k_BT}{M\eta_s}\sum_{p=1}^{N}\frac{\tau_p}{2} = \frac{N_{\mathrm{Av}}}{M}12\pi\left[\frac{(N+1)b^2}{12\pi}\right]^{\frac{3}{2}}\sum_{p=1}^{N}\frac{1}{p^{\frac{3}{2}}}, \tag{3.20}$$

where ρ is the polymer concentration and M is the mol mass of the polymer. The intrinsic viscosity scales with $N^{1/2}$ (remember that $M \propto N$), again in agreement with experiments on dilute polymer solutions.

Problems

3-1. Proof the last step in Eq. (3.7) [Hint: the Zimm chain is a Gaussian chain].
3-2. Check Eq. (3.18) explicitly from Eqs. (3.12) and (3.16) and by noting that

$$0 = \frac{\mathrm{d}}{\mathrm{d}t}\left\langle \mathbf{X}_p(t)\cdot\mathbf{X}_p(t)\right\rangle = -\frac{2}{\tau_p}\left\langle \mathbf{X}_p(t)\cdot\mathbf{X}_p(t)\right\rangle + 2\left\langle \mathbf{F}_p(t)\cdot\mathbf{X}_p(t)\right\rangle$$

in equilibrium, where the last term is equal to

$$2\int_0^t \mathrm{d}\tau\,\mathrm{e}^{-(t-\tau)/\tau_p}\left\langle \mathbf{F}_p(t)\cdot\mathbf{F}_p(\tau)\right\rangle = \int_{-\infty}^{\infty}\mathrm{d}\tau\,\mathrm{e}^{-|t-\tau|/\tau_p}\left\langle \mathbf{F}_p(t)\cdot\mathbf{F}_p(\tau)\right\rangle.$$

3-3. Proof the first step in Eq. (3.19). [Hint: remember that the centre-of-mass is given by $\mathbf{X}_0$].

Appendix A: Derivation of hydrodynamic interactions in a suspension of spheres

In Appendix A of chapter 2 we calculated the flow field in the solvent around a *single* slowly moving sphere. When more than one sphere is present in the system, this flow field will be felt by the other spheres. As a result these spheres experience a force which is said to result from hydrodynamic interactions with the original sphere.

We will assume that at each time the fluid flow field can be treated as a steady state flow field. This is true for very slow flows, where changes in positions and velocities of the spheres take place over much larger time scales than the time it takes for the fluid flow field to react to such changes. The hydrodynamic problem then is to find a flow field satisfying the stationary Stokes equations,

$$\eta_s \nabla^2 \mathbf{v} = \boldsymbol{\nabla} P \tag{A.1}$$

$$\boldsymbol{\nabla} \cdot \mathbf{v} = 0, \tag{A.2}$$

together with the boundary conditions

$$\mathbf{v}(\mathbf{R}_i + \mathbf{a}) = \mathbf{v}_i \qquad \forall i, \tag{A.3}$$

where $\mathbf{R}_i$ is the position vector and $\mathbf{v}_i$ is the velocity vector of the i'th sphere, and $\mathbf{a}$ is any vector of length a. If the spheres are very far apart we may approximately consider any one of them to be alone in the fluid. The flow field is then just the sum of all flow fields emanating from the different spheres

$$\mathbf{v}(\mathbf{r}) = \sum_i \mathbf{v}_i^{(0)}(\mathbf{r} - \mathbf{R}_i), \tag{A.4}$$

where, according to Eq. (A.13),

$$\mathbf{v}_i^{(0)}(\mathbf{r} - \mathbf{R}_i) = \mathbf{v}_i \frac{3a}{4|\mathbf{r} - \mathbf{R}_i|}\left[1 + \frac{a^2}{3(\mathbf{r} - \mathbf{R}_i)^2}\right] + (\mathbf{r} - \mathbf{R}_i)((\mathbf{r} - \mathbf{R}_i) \cdot \mathbf{v}_i)\frac{3a}{4|\mathbf{r} - \mathbf{R}_i|^3}\left[1 - \frac{a^2}{(\mathbf{r} - \mathbf{R}_i)^2}\right]. \tag{A.5}$$

We shall now calculate the correction to this flow field, which is of lowest order in the sphere separation.

We shall first discuss the situation for only two spheres in the fluid. In the neighbourhood of sphere one the velocity field may be written as

$$\mathbf{v}(\mathbf{r}) = \mathbf{v}_1^{(0)}(\mathbf{r} - \mathbf{R}_1) + \frac{3a}{4|\mathbf{r} - \mathbf{R}_2|}\left[\mathbf{v}_2 + \frac{(\mathbf{r} - \mathbf{R}_2)}{|\mathbf{r} - \mathbf{R}_2|}\frac{(\mathbf{r} - \mathbf{R}_2)}{|\mathbf{r} - \mathbf{R}_2|} \cdot \mathbf{v}_2\right], \tag{A.6}$$

where we have approximated $\mathbf{v}_2^{(0)}(\mathbf{r}-\mathbf{R}_2)$ to terms of order $a/|\mathbf{r}-\mathbf{R}_2|$. On the surface of sphere one we approximate this further by

$$\mathbf{v}(\mathbf{R}_1+\mathbf{a}) = \mathbf{v}_1^{(0)}(\mathbf{a}) + \frac{3a}{4R_{21}}\left(\mathbf{v}_2 + \hat{\mathbf{R}}_{21}\hat{\mathbf{R}}_{21}\cdot\mathbf{v}_2\right), \tag{A.7}$$

where $\hat{\mathbf{R}}_{21} = (\mathbf{R}_2-\mathbf{R}_1)/|\mathbf{R}_2-\mathbf{R}_1|$. Because $\mathbf{v}_1^{(0)}(\mathbf{a}) = \mathbf{v}_1$, we notice that this result is not consistent with the boundary condition $\mathbf{v}(\mathbf{R}_1+\mathbf{a}) = \mathbf{v}_1$. In order to satisfy this boundary condition we subtract from our results so far, a solution of Eqs. (A.1) and (A.2) which goes to zero at infinity, and which on the surface of sphere one corrects for the second term in Eq. (A.7). The flow field in the neighbourhood of sphere one then reads

$$\begin{aligned}
\mathbf{v}(\mathbf{r}) &= \mathbf{v}_1^{\mathrm{corr}}\frac{3a}{4|\mathbf{r}-\mathbf{R}_1|}\left[1+\frac{a^2}{3(\mathbf{r}-\mathbf{R}_1)^2}\right] \\
&\quad +(\mathbf{r}-\mathbf{R}_1)((\mathbf{r}-\mathbf{R}_1)\cdot\mathbf{v}_1^{\mathrm{corr}})\frac{3a}{4|\mathbf{r}-\mathbf{R}_1|^3}\left[1-\frac{a^2}{(\mathbf{r}-\mathbf{R}_1)^2}\right] \\
&\quad +\frac{3a}{4R_{21}}\left(\mathbf{v}_2+\hat{\mathbf{R}}_{21}\hat{\mathbf{R}}_{21}\cdot\mathbf{v}_2\right) \qquad \text{(A.8)} \\
\mathbf{v}_1^{\mathrm{corr}} &= \mathbf{v}_1 - \frac{3a}{4R_{21}}\left(\mathbf{v}_2+\hat{\mathbf{R}}_{21}\hat{\mathbf{R}}_{21}\cdot\mathbf{v}_2\right). \qquad \text{(A.9)}
\end{aligned}$$

The flow field in the neighbourhood of sphere two is treated similarly.

We notice that the correction that we have applied to the flow field in order to satisfy the boundary conditions at the surface of sphere one is of order a/R_{21}. Its strength in the neighbourhood of sphere two is then of order $(a/R_{21})^2$, and need therefore not be taken into account when the flow field is adapted to the boundary conditions at sphere two.

The flow field around sphere one is now given by Eqs. (A.8) and (A.9). The last term in Eq. (A.8) does not contribute to the stress tensor (the gradient of a constant field is zero). The force exerted by the fluid on sphere one then equals $-6\pi\eta_s a\mathbf{v}_1^{\mathrm{corr}}$. A similar result holds for sphere two. In full we have

$$\begin{aligned}
\mathbf{F}_1 &= -6\pi\eta_s a\mathbf{v}_1 + 6\pi\eta_s a\frac{3a}{4R_{21}}\left(\bar{\mathbf{I}}+\hat{\mathbf{R}}_{21}\hat{\mathbf{R}}_{21}\right)\cdot\mathbf{v}_2 \qquad \text{(A.10)} \\
\mathbf{F}_2 &= -6\pi\eta_s a\mathbf{v}_2 + 6\pi\eta_s a\frac{3a}{4R_{21}}\left(\bar{\mathbf{I}}+\hat{\mathbf{R}}_{21}\hat{\mathbf{R}}_{21}\right)\cdot\mathbf{v}_1, \qquad \text{(A.11)}
\end{aligned}$$

where $\bar{\mathbf{I}}$ is the three-dimensional unit tensor. Inverting these equations, retaining only terms up to order a/R_{21}, we get

$$\mathbf{v}_1 = -\frac{1}{6\pi\eta_s a}\mathbf{F}_1 - \frac{1}{8\pi\eta_s R_{21}}\left(\bar{\mathbf{I}}+\hat{\mathbf{R}}_{21}\hat{\mathbf{R}}_{21}\right)\cdot\mathbf{F}_2 \tag{A.12}$$

$$\mathbf{v}_2 = -\frac{1}{6\pi\eta_s a}\mathbf{F}_2 - \frac{1}{8\pi\eta_s R_{21}}\left(\bar{\mathbf{I}}+\hat{\mathbf{R}}_{21}\hat{\mathbf{R}}_{21}\right)\cdot\mathbf{F}_1 \tag{A.13}$$

When more than two spheres are present in the fluid, corrections resulting from n-body interactions ($n \geq 3$) are of order $(a/R_{ij})^2$ or higher and need not be taken into account. The above treatment therefore generalizes to

$$\mathbf{F}_i = -\sum_{j=0}^{N} \bar{\boldsymbol{\zeta}}_{ij} \cdot \mathbf{v}_j \tag{A.14}$$

$$\mathbf{v}_i = -\sum_{j=0}^{N} \bar{\boldsymbol{\mu}}_{ij} \cdot \mathbf{F}_j, \tag{A.15}$$

where

$$\bar{\boldsymbol{\zeta}}_{ii} = 6\pi\eta_s a \bar{\mathbf{I}}, \qquad \bar{\boldsymbol{\zeta}}_{ij} = -6\pi\eta_s a \frac{3a}{4R_{ij}} \left(\bar{\mathbf{I}} + \hat{\mathbf{R}}_{ij}\hat{\mathbf{R}}_{ij}\right) \tag{A.16}$$

$$\bar{\boldsymbol{\mu}}_{ii} = \frac{1}{6\pi\eta_s a}\bar{\mathbf{I}}, \qquad \bar{\boldsymbol{\mu}}_{ij} = \frac{1}{8\pi\eta_s R_{ij}} \left(\bar{\mathbf{I}} + \hat{\mathbf{R}}_{ij}\hat{\mathbf{R}}_{ij}\right). \tag{A.17}$$

$\bar{\boldsymbol{\mu}}_{ij}$ is generally called the mobility tensor. The specific form Eq. (A.17) is known as the Oseen tensor.

Appendix B: Smoluchowski equation for the Zimm chain

For sake of completeness, we will describe the Smoluchowski equation for the beads in a Zimm chain. The equation is similar to, but a generalized version of, the Smoluchowski equation for a single bead treated in Appendix B of chapter 2.

Let $\Psi(\mathbf{R}_0, \ldots, \mathbf{R}_N; t)$ be the probability density of finding beads $0, \ldots, N$ near $\mathbf{R}_0, \ldots, \mathbf{R}_N$ at time t. The equation of particle conservation can be written as

$$\frac{\partial \Psi}{\partial t} = -\sum_{j=0}^{N} \boldsymbol{\nabla}_j \cdot \mathbf{J}_j, \tag{B.1}$$

where $\mathbf{J}_j$ is the flux of beads j. This flux may be written as

$$\mathbf{J}_j = -\sum_k \bar{\mathbf{D}}_{jk} \cdot \boldsymbol{\nabla}_k \Psi - \sum_k \bar{\boldsymbol{\mu}}_{jk} \cdot (\boldsymbol{\nabla}_k \Phi)\, \Psi. \tag{B.2}$$

The first term in Eq. (B.2) is the flux due to the random displacements of all beads, which results in a flux along the negative gradient of the probability density. The second term results from the forces $-\boldsymbol{\nabla}_k \Phi$ felt by all the beads. On the Smoluchowski time scale, these forces make the beads move with constant velocities $\mathbf{v}_k$, i.e., the forces $-\boldsymbol{\nabla}_k \Phi$ are exactly balanced by the hydrodynamic forces acting on

the beads k. Introducing these forces into Eq. (A.15), we find the systematic part of the velocity of bead j:

$$\mathbf{v}_j = -\sum_k \bar{\boldsymbol{\mu}}_{jk} \cdot (\boldsymbol{\nabla}_k \Phi). \tag{B.3}$$

Multiplying this by Ψ, we obtain the systematic part of the flux of particle j.

At equilibrium, each flux $\mathbf{J}_j$ must be zero and the distribution must be equal to the Boltzmann distribution $\Psi_{\rm eq} = C\exp[-\beta\Phi]$. Using this in Eq. (B.2) it follows that

$$\bar{\mathbf{D}}_{jk} = k_B T \bar{\boldsymbol{\mu}}_{jk}, \tag{B.4}$$

which is a generalization of the Einstein equation.

Combining Eqs. (B.1), (B.2), and (B.4) we find the Smoluchowski equation for the beads in a Zimm chain:

$$\frac{\partial \Psi}{\partial t} = \sum_j \sum_k \boldsymbol{\nabla}_j \cdot \bar{\boldsymbol{\mu}}_{jk} \cdot (\boldsymbol{\nabla}_k \Phi + k_B T \boldsymbol{\nabla}_k \ln \Psi)\, \Psi. \tag{B.5}$$

Using techniques similar to those used in Appendix B of chapter 2, it can be shown that the Langevin Eqs. (3.3) - (3.5) are equivalent to the above Smoluchowski equation.

Appendix C: Derivation of Eq. (3.12)

In order to derive Eq. (3.12) we write

$$\begin{aligned}
\mu_{pq} &= \frac{2}{N+1}\frac{1}{6\pi\eta_s b}\sqrt{\frac{6}{\pi}}\sum_{j=0}^{N}\cos\left[\frac{p\pi}{N+1}(j+\frac{1}{2})\right]\times \\
&\quad \sum_{k=j-N}^{j}\cos\left[\frac{q\pi}{N+1}(j-k+\frac{1}{2})\right]\frac{1}{\sqrt{|k|}} \\
&= \frac{2}{N+1}\frac{1}{6\pi\eta_s b}\sqrt{\frac{6}{\pi}}\sum_{j=0}^{N}\cos\left[\frac{p\pi}{N+1}(j+\frac{1}{2})\right]\cos\left[\frac{q\pi}{N+1}(j+\frac{1}{2})\right]\times \\
&\quad \sum_{k=j-N}^{j}\cos\left(\frac{q\pi k}{N+1}\right)\frac{1}{\sqrt{|k|}} \\
&\quad +\frac{2}{N+1}\frac{1}{6\pi\eta_s b}\sqrt{\frac{6}{\pi}}\sum_{j=0}^{N}\cos\left[\frac{p\pi}{N+1}(j+\frac{1}{2})\right]\sin\left[\frac{q\pi}{N+1}(j+\frac{1}{2})\right]\times \\
&\quad \sum_{k=j-N}^{j}\sin\left(\frac{q\pi k}{N+1}\right)\frac{1}{\sqrt{|k|}}.
\end{aligned} \tag{C.1}$$

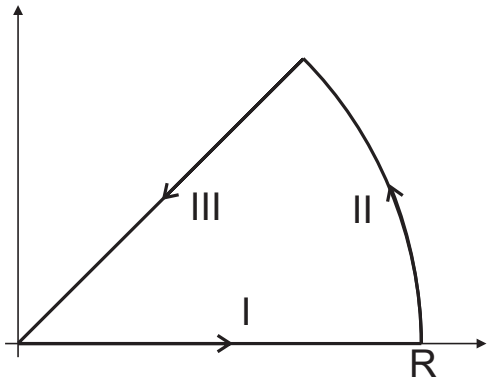

Figure 3.1: Contour for integration in the complex plane, Eq. (C.4). Part I is a line along the real axis from $x = 0$ to $x = R$, part II is a semicircle $z = Re^{i\phi}$, where $\phi \in]0, \pi/4]$, and part III is the diagonal line $z = (1+\mathrm{i})x$, where $x \in]0, R/\sqrt{2}]$.

We now approximate

$$\sum_{k=j-N}^{j} \cos\left(\frac{q\pi k}{N+1}\right)\frac{1}{\sqrt{|k|}} \approx \int_{-\infty}^{\infty} \mathrm{d}k\, \cos\left(\frac{q\pi k}{N+1}\right)\frac{1}{\sqrt{|k|}}$$
$$= 4\int_0^{\infty} \mathrm{d}x\, \cos\left(\frac{q\pi x^2}{N+1}\right) = \sqrt{\frac{2(N+1)}{q}} \quad \text{(C.2)}$$

$$\sum_{k=j-N}^{j} \sin\left(\frac{q\pi k}{N+1}\right)\frac{1}{\sqrt{|k|}} \approx \int_{-\infty}^{\infty} \mathrm{d}k\, \sin\left(\frac{q\pi k}{N+1}\right)\frac{1}{\sqrt{|k|}} = 0. \quad \text{(C.3)}$$

The result of Eq. (C.3) is obvious because the integrand is an odd function of k. The last equality in Eq. (C.2) can be found by considering the complex function $f(z) = \exp(\mathrm{i}az^2)$ for any positive real number a on the contour given in Fig. 3.1. Because $f(z)$ is analytic (without singularities) on all points on and within the contour, the contour integral of $f(z)$ must be zero. We now write

$$\begin{aligned} 0 &= \oint \mathrm{d}z\, \mathrm{e}^{\mathrm{i}az^2} = \int_{(\mathrm{I})} \mathrm{d}z\, \mathrm{e}^{\mathrm{i}az^2} + \int_{(\mathrm{II})} \mathrm{d}z\, \mathrm{e}^{\mathrm{i}az^2} + \int_{(\mathrm{III})} \mathrm{d}z\, \mathrm{e}^{\mathrm{i}az^2} \\ &= \int_0^R \mathrm{d}x\, \mathrm{e}^{\mathrm{i}ax^2} + \int_0^{\pi/4} \mathrm{d}\phi\, \mathrm{i}R\mathrm{e}^{\mathrm{i}\phi + \mathrm{i}aR^2\mathrm{e}^{2\mathrm{i}\phi}} + \int_{R/\sqrt{2}}^0 \mathrm{d}x\, (1+\mathrm{i})\mathrm{e}^{\mathrm{i}a[(1+\mathrm{i})x]^2} \\ &= \int_0^R \mathrm{d}x\, \mathrm{e}^{\mathrm{i}ax^2} + \int_0^{\pi/4} \mathrm{d}\phi\, \mathrm{i}R\mathrm{e}^{\mathrm{i}\phi + \mathrm{i}aR^2\cos 2\phi - aR^2\sin 2\phi} - (1+\mathrm{i})\int_0^{R/\sqrt{2}} \mathrm{d}x\, \mathrm{e}^{-2ax^2} \end{aligned} \quad \text{(C.4)}$$

Taking the limit $R \to \infty$ the second term vanishes, after which the real part of the equation yields

$$\int_0^{\infty} \mathrm{d}x\, \cos(ax^2) = \int_0^{\infty} \mathrm{d}x\, \mathrm{e}^{-2ax^2} = \sqrt{\frac{\pi}{8a}}. \quad \text{(C.5)}$$

Introducing Eqs. (C.2) and (C.3) into Eq. (C.1) one finds Eq. (3.12). As a technical detail we note that in principle diagonal terms in Eq. (3.11) should have

been treated separately, which is clear from Eq. (A.17). Since the contribution of all other terms is proportional to $N^{1/2}$, however, we omit the diagonal terms.

Chapter 4

The tube model

4.1 Entanglements in dense polymer systems

In the Rouse model we have assumed that interactions between different chains can be treated through some effective friction coefficient. As we have seen, this model applies well to melts of short polymer chains. In the Zimm model we have assumed that interactions between different chains can be ignored altogether, and only *intra*chain hydrodynamic interactions need to be taken into account. This model applies well to dilute polymer systems.

We will now treat the case of long polymer chains at high concentration or in the melt state. Studies of the mechanical properties of such systems reveal a nontrivial molecular weight dependence of the viscosity and rubber-like elastic behavior on time scales which increase with chain length. The observed behavior is rather universal, independent of temperature or molecular species (as long as the polymer is linear and flexible), which indicates that the phenomena are governed by the general nature of polymers. This general nature is, of course, the fact that the chains are intertwined and can not penetrate through each other: they are "entangled" (see Fig. 4.1). These topological interactions seriously affect the dynamical properties since they impose constraints on the motion of the polymers.

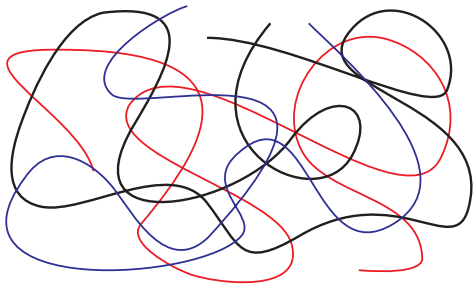

Figure 4.1: A simplified picture of polymer chains at high density. The chains are intertwined and cannot penetrate through each other.

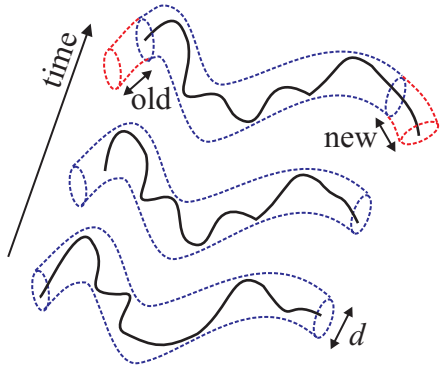

Figure 4.2: Representation of a polymer in a tube. The tube is due to surrounding chains, i.e. entanglements, so that the polymer can only reptate along the tube.

4.2 The tube model

In the tube model, introduced by De Gennes and further refined by Doi and Edwards, the complicated topological interactions are simplified to an effective tube surrounding each polymer chain. In order to move over large distances, the chain has to leave the tube by means of longitudinal motions. This concept of a tube clearly has only a statistical (mean field) meaning. The tube can change by two mechanisms. First by means of the motion of the central chain itself, by which the chain leaves parts of its original tube, and generates new parts. Secondly, the tube will fluctuate because of motions of the chains which build up the tube. It is generally believed that tube fluctuations of the second kind are unimportant for extremely long chains. For the case of medium long chains, subsequent corrections can be made to account for fluctuating tubes.

Let us now look at the mechanisms which allow the polymer chain to move along the tube axis, which is also called the primitive chain.

The chain of interest fluctuates around the primitive chain. By some fluctuation it may store some excess mass in part of the chain, see Fig. 4.2. This mass may diffuse along the primitive chain and finally leave the tube. The chain thus creates a new piece of tube and at the same time destroys part of the tube at the other side. This kind of motion is called *reptation*. Whether the tube picture is indeed correct for concentrated polymer solutions or melts still remains a matter for debate, but many experimental and simulation results suggest that reptation is the dominant mechanism for the dynamics of a chain in the highly entangled state.

It is clear from the above picture that the reptative motion will determine the long time motion of the chain. The main concept of the model is the primitive chain. The details of the polymer itself are to a high extent irrelevant. We may therefore choose a convenient polymer as we wish. Our polymer will again be a Gaussian chain. Its motion will be governed by the Langevin equations at the Smoluchowski time scale. Our basic chain therefore is a Rouse chain.

4.3 Definition of the model

The tube model consists of two parts. First we have the basic chain, and secondly we have the tube and its motion. So:

- Basic chain
  Rouse chain with parameters N, b and ζ.
- Primitive chain

  1. The primitive chain has contour length L, which is assumed to be constant. The position along the primitive chain will be indicated by the continuous variable $s \in [0,L]$. The configurations of the primitive chain are assumed to be Gaussian; by this we mean that

     $$\left\langle \left(\mathbf{R}(s)-\mathbf{R}(s')\right)^2 \right\rangle = d\left|s-s'\right|, \tag{4.1}$$

     where d is a new parameter having the dimensions of length. It is the step length of the primitive chain, or the tube diameter.
  2. The primitive chain can move back and forth only along itself with diffusion coefficient

     $$D_G = \frac{k_B T}{(N+1)\zeta}, \tag{4.2}$$

     i.e., with the Rouse diffusion coefficient, because the motion of the primitive chain corresponds to the overall translation of the Rouse chain along the tube.

The Gaussian character of the distribution of primitive chain conformations is consistent with the reptation picture, in which the chain continuously creates new pieces of tube, which may be chosen in random directions with step length d.

Apparently we have introduced two new parameters, the contour length L and the step length d. Only one of them is independent, however, because they are related by the end-to-end distance of the chain, $\left\langle R^2 \right\rangle = Nb^2 = dL$, where the first equality stems from the fact that we are dealing with a Rouse chain, and the second equality follows from Eq. (4.1).

4.4 Segmental motion

We shall now demonstrate that according to our model the mean quadratic displacement of a typical monomer behaves like in Fig. (4.3). This behaviour has

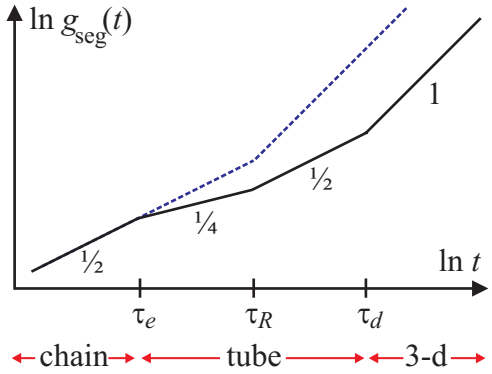

Figure 4.3: Logarithmic plot of the segmental mean square displacement, in case of the reptation model (solid line) and the Rouse model (dashed line).

been qualitatively verified by computer simulations. Of course the final regime should be simple diffusive motion. The important prediction is the dependence of the diffusion constant on N.

In Fig. (4.3), τ_R is the Rouse time which is equal to τ_1 in Eq. (2.46). The meaning of τ_e and τ_d will become clear in the remaining part of this section. We shall now treat the different regimes in Fig. (4.3) one after another.

i) $t \leq \tau_e$

At short times a Rouse bead does not know about any tube constraints. According to Eq. (2.57) then

$$g_{\text{seg}}(t) = \left(\frac{12kTb^2}{\pi\zeta}\right)^{\frac{1}{2}} t^{\frac{1}{2}}. \tag{4.3}$$

Once the segment has moved a distance equal to the tube diameter d, it will feel the constraints of the tube, and a new regime will set in. The time at which this happens is given by the entanglement time

$$\tau_e = \frac{\pi\zeta}{12k_BTb^2}d^4. \tag{4.4}$$

Notice that this is independent of N.

ii) $\tau_e < t \leq \tau_R$

On the time and distance scale we are looking now, the bead performs random motions, still constrained by the fact that the monomer is a part of a chain because $t \leq \tau_R$. Orthogonally to the primitive chain these motions do not lead to any displacement, because of the constraints implied by the tube. Only along the primitive chain the bead may diffuse free of any other constraint than the one

implied by the fact that it belongs to a chain. The diffusion therefore is given by the 1-dimensional analog of Eq. (2.57) or Eq. (4.3),

$$\left\langle (s_n(t) - s_n(0))^2 \right\rangle = \frac{1}{3} \left(\frac{12kTb^2}{\pi\zeta} \right)^{\frac{1}{2}} t^{\frac{1}{2}}, \tag{4.5}$$

where $s_n(t)$ is the position of bead n along the primitive chain at time t. It is assumed here that for times $t \leq \tau_R$ the chain as a whole does not move, i.e. that the primitive chain does not change. Using Eq. (4.1) then

$$g_{\text{seg}}(t) = d \left(\frac{4k_BTb^2}{3\pi\zeta} \right)^{\frac{1}{4}} t^{\frac{1}{4}}, \tag{4.6}$$

where we have assumed $\langle |s_n(t) - s_n(0)| \rangle \approx \left\langle (s_n(t) - s_n(0))^2 \right\rangle^{\frac{1}{2}}$.

iii) $\tau_R < t \leq \tau_d$

The bead still moves along the tube diameter. Now however $t > \tau_R$, which means that we should use the 1-dimensional analog of Eq. (2.56):

$$\left\langle (s_n(t) - s_n(0))^2 \right\rangle = 2D_G t. \tag{4.7}$$

Again assuming that the tube does not change appreciably during time t, we get

$$g_{\text{seg}}(t) = d \left[\frac{2k_BT}{(N+1)\zeta} \right]^{\frac{1}{2}} t^{\frac{1}{2}}. \tag{4.8}$$

From our treatment it is clear that τ_d is the time it takes for the chain to create a tube which is uncorrelated to the old one, or the time it takes for the chain to get disentangled from its old surroundings. We will calculate the disentanglement time τ_d in the next paragraph.

iv) $\tau_d < t$

This is the regime in which reptation dominates. On this time and space scale we may attribute to every bead a definite value of s. We then want to calculate

$$\varphi(s,t) = \langle (\mathbf{R}(s,t) - \mathbf{R}(s,0))^2 \rangle, \tag{4.9}$$

where $\mathbf{R}(s,t)$ is the position of bead s at time t. In order to calculate $\varphi(s,t)$ it is useful to introduce

$$\varphi(s,s';t) = \left\langle (\mathbf{R}(s,t) - \mathbf{R}(s',0))^2 \right\rangle, \tag{4.10}$$

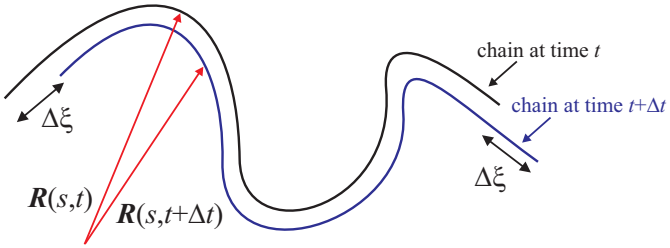

Figure 4.4: Motion of the primitive chain along its contour.

i.e. the mean square distance between bead s at time t and bead s' at time zero. According to Fig. (4.4), for all s, except $s = 0$ and $s = L$, we have

$$\varphi(s,s';t+\Delta t) = \left\langle \varphi(s+\Delta\xi,s';t)\right\rangle, \tag{4.11}$$

where $\Delta\xi$ according to the definition of the primitive chain in section 4.3 is a stochastic variable. The average on the right hand side has to be taken over the distribution of $\Delta\xi$. Expanding the right hand side of Eq. (4.11) we get

$$\begin{aligned}\left\langle \varphi(s+\Delta\xi,s';t)\right\rangle &\approx \varphi(s,s';t) + \langle\Delta\xi\rangle\frac{\partial}{\partial s}\varphi(s,s';t) + \frac{1}{2}\left\langle(\Delta\xi)^2\right\rangle\frac{\partial^2}{\partial s^2}\varphi(s,s';t)\\ &= \varphi(s,s';t) + D_G\Delta t\frac{\partial^2}{\partial s^2}\varphi(s,s';t).\end{aligned} \tag{4.12}$$

Introducing this into Eq. (4.11) and taking the limit for Δt going to zero, we get

$$\frac{\partial}{\partial t}\varphi(s,s';t) = D_G\frac{\partial^2}{\partial s^2}\varphi(s,s';t). \tag{4.13}$$

In order to complete our description of reptation we have to find the boundary conditions going with this diffusion equation. We will demonstrate that these are given by

$$\varphi(s,s';t)|_{t=0} = d|s-s'| \tag{4.14}$$

$$\frac{\partial}{\partial s}\varphi(s,s';t)|_{s=L} = d \tag{4.15}$$

$$\frac{\partial}{\partial s}\varphi(s,s';t)|_{s=0} = -d. \tag{4.16}$$

The first of these is obvious. The second follows from

$$\begin{aligned}
\frac{\partial}{\partial s}\varphi(s,s';t)|_{s=L} &= 2\left\langle \frac{\partial \mathbf{R}(s,t)}{\partial s}|_{s=L}\cdot(\mathbf{R}(L,t)-\mathbf{R}(s',0))\right\rangle \\
&= 2\left\langle \frac{\partial \mathbf{R}(s,t)}{\partial s}|_{s=L}\cdot(\mathbf{R}(L,t)-\mathbf{R}(s',t))\right\rangle \\
&\quad +2\left\langle \frac{\partial \mathbf{R}(s,t)}{\partial s}|_{s=L}\cdot(\mathbf{R}(s',t)-\mathbf{R}(s',0))\right\rangle \\
&= 2\left\langle \frac{\partial \mathbf{R}(s,t)}{\partial s}|_{s=L}\cdot(\mathbf{R}(L,t)-\mathbf{R}(s',t))\right\rangle \\
&= \frac{\partial}{\partial s}\left\langle(\mathbf{R}(s,t)-\mathbf{R}(s',t))^2\right\rangle|_{s=L} = \frac{\partial}{\partial s}d|s-s'|_{s=L}. \qquad (4.17)
\end{aligned}$$

Condition Eq. (4.16) follows from a similar reasoning.

We now solve Eqs. (4.13)–(4.16), obtaining

$$\begin{aligned}
\varphi(s,s';t) &= |s-s'|d+2D_G\frac{d}{L}t \\
&\quad +4\frac{Ld}{\pi^2}\sum_{p=1}^{\infty}\frac{1}{p^2}(1-\mathrm{e}^{-tp^2/\tau_d})\cos\left(\frac{p\pi s}{L}\right)\cos\left(\frac{p\pi s'}{L}\right), \qquad (4.18)
\end{aligned}$$

where

$$\tau_d = \frac{L^2}{\pi^2 D_G} = \frac{1}{\pi^2}\frac{b^4}{d^2}\frac{\zeta}{k_BT}N^3. \qquad (4.19)$$

We shall not derive this here. The reader may check that Eq. (4.18) indeed is the solution to Eq. (4.13) satisfying (4.14)-(4.16).

Notice that τ_d becomes much larger than τ_R for large N, see Eq. (2.46). If the number of steps in the primitive chain is defined by $Z = Nb^2/d^2 = L/d$, then the ratio between τ_d and τ_R is $3Z$.

Taking the limit $s \to s'$ in Eq. (4.18) we get

$$\left\langle(\mathbf{R}(s,t)-\mathbf{R}(s,0))^2\right\rangle = 2D_G\frac{d}{L}t+4\frac{Ld}{\pi^2}\sum_{p=1}^{\infty}\cos^2\left(\frac{p\pi s}{L}\right)(1-e^{-tp^2/\tau_d})\frac{1}{p^2}. \qquad (4.20)$$

For $t > \tau_d$ we get diffusive behaviour with diffusion constant

$$D = \frac{1}{3}D_G\frac{d}{L} = \frac{1}{3}\frac{d^2}{b^2}\frac{k_BT}{\zeta}\frac{1}{N^2}. \qquad (4.21)$$

Notice that this is proportional to N^{-2}, whereas the diffusion coefficient of the Rouse model was proportional to N^{-1}. The reptation result, N^{-2}, is confirmed by experiments which measured the diffusion coefficients of polymer melts as a function of their molecular weight.

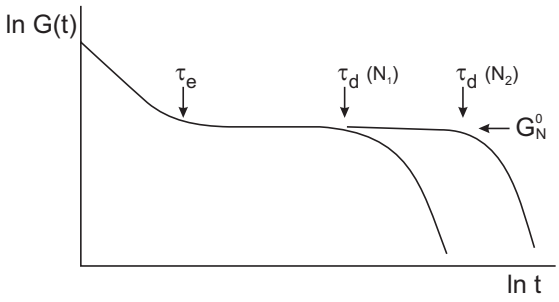

Figure 4.5: Schematic logaritmic plot of the time behaviour of the shear relaxation modulus $G(t)$ as measured in a concentated polymer solution or melt; $N_1 < N_2$.

4.5 Viscoelastic behaviour

Experimentally the shear relaxation modulus $G(t)$ of a concentrated polymer solution or melt turns out to be like in Fig. 4.5. We distinguish two regimes.

i) $t < \tau_e$

At short times the chain behaves like a 3-dimensional Rouse chain. Using Eq. (2.79) we find

$$\begin{aligned} G(t) &= \frac{ck_BT}{N+1}\sum_{p=1}^{N}\exp\left(-2t/\tau_p\right) \\ &\approx \frac{ck_BT}{N+1}\int_0^\infty \mathrm{d}p\ \exp\left(-2p^2t/\tau_R\right) \\ &= \frac{ck_BT}{N+1}\sqrt{\frac{\pi\tau_R}{8t}}, \end{aligned} \tag{4.22}$$

which decays as $t^{-\frac{1}{2}}$. At $t = \tau_e$ this possibility to relax ends. The only way for the chain to relax any further is by breaking out of the tube.

ii) $t > \tau_e$

The stress that remains in the system is caused by the fact that the chains are trapped in twisted tubes. By means of reptation the chain can break out of its tube. The newly generated tube contains no stress. So, it is plausible to assume that the stress at any time t is proportional to the fraction of the original tube that is still part of the tube at time t. We'll call this fraction $\Psi(t)$. So,

$$G(t) = G_N^0\Psi(t). \tag{4.23}$$

On the reptation time scale, τ_e is practically zero, so we can set $\Psi(\tau_e) = \Psi(0) = 1$. To make a smooth transition from the Rouse regime to the reptation regime, we

match Eq. (4.22) with Eq. (4.23) at $t = \tau_e$, yielding

$$G_N^0 = \frac{ck_BT}{N+1}\sqrt{\frac{\pi\tau_R}{8\tau_e}} = \frac{ck_BT}{\sqrt{2}\pi}\frac{b^2}{d^2}. \tag{4.24}$$

Notice that the plateau value G_N^0 is independent of the chain length N. The numerical prefactor of $1/\sqrt{2}\pi$ in Eq. (4.24) is not rigorous because in reptation theory the time τ_e, at which the Rouse-like modulus is supposed to be instantaneously replaced by the reptation-like modulus, is not defined in a rigorous manner. A more precise calculation based on stress relaxation after a large step strain gives a numerical prefactor of 4/5, i.e.

$$G_N^0 = \frac{4}{5}\frac{ck_BTb^2}{d^2} = \frac{4}{5}\frac{ck_BT}{N_e}. \tag{4.25}$$

In the last equation we have defined the entanglement length N_e. In most experiments the entanglement length (or more precisely the entanglement molecular weight) is estimated from the value of the plateau modulus, using Eq. (4.25).

We will now calculate $\Psi(t)$. Take a look at

$$\left\langle \mathbf{u}\left(s',t\right)\cdot\mathbf{u}\left(s,0\right)\right\rangle \equiv \left\langle \frac{\partial\mathbf{R}\left(s',t\right)}{\partial s'}\cdot\frac{\partial\mathbf{R}\left(s,0\right)}{\partial s}\right\rangle. \tag{4.26}$$

The vector $\mathbf{u}(s',t)$ is the tangent to the primitive chain, at segment s' at time t. Because the primitive chain has been parametrized with the contour length, we have from Eq. (4.1) $\langle \mathbf{u}\cdot\mathbf{u}\rangle = \langle \Delta\mathbf{R}\cdot\Delta\mathbf{R}\rangle / (\Delta s)^2 = d/\Delta s$; the non-existence of the limit of $\triangle s$ going to zero is a peculiarity of a Gaussian process. Using Eqs. (4.10) and (4.18) we calculate

$$\begin{aligned}
\left\langle \mathbf{u}\left(s',t\right)\cdot\mathbf{u}\left(s,0\right)\right\rangle &= -\frac{1}{2}\frac{\partial^2}{\partial s\partial s'}\varphi\left(s',s;t\right)\\
&= d\delta\left(s-s'\right) - \frac{2d}{L}\sum_{p=1}^{\infty}\left(1-\mathrm{e}^{-tp^2/\tau_d}\right)\sin\left(\frac{p\pi s}{L}\right)\sin\left(\frac{p\pi s'}{L}\right)\\
&= \frac{2d}{L}\sum_{p=1}^{\infty}\mathrm{e}^{-tp^2/\tau_d}\sin\left(\frac{p\pi s}{L}\right)\sin\left(\frac{p\pi s'}{L}\right),
\end{aligned} \tag{4.27}$$

where we have used

$$\frac{2}{L}\sum_{p=1}^{\infty}\sin\left(\frac{p\pi s}{L}\right)\sin\left(\frac{p\pi s'}{L}\right) = \delta\left(s-s'\right). \tag{4.28}$$

Using this last equation, we also find

$$\left\langle \mathbf{u}\left(s',0\right)\cdot\mathbf{u}\left(s,0\right)\right\rangle = d\delta\left(s-s'\right). \tag{4.29}$$

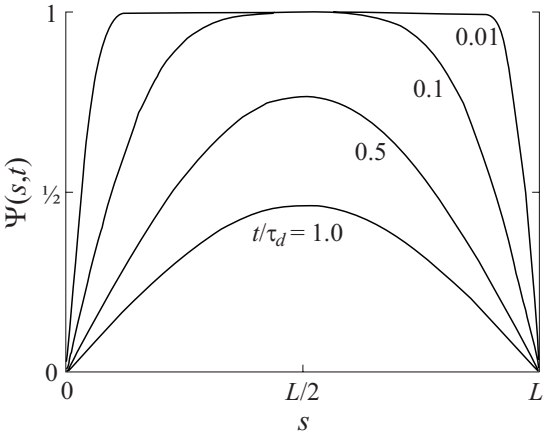

Figure 4.6: Development of $\Psi(s,t)$ in time.

This equation states that there is no correlation between the tangents to the primitive chain at a segment s, and at another segment s'. If we consider $\langle \mathbf{u}(s',t)\cdot\mathbf{u}(s,0)\rangle$ as a function of s', at time t, we see that the original delta function has broadened and lowered. However, the tangent $\mathbf{u}(s',t)$ can only be correlated to $\mathbf{u}(s,0)$ by means of diffusion of segment s', during the time interval $[0,t]$, to the place where s was at time $t=0$, and still lies in the original tube. So, $\frac{1}{d}\langle \mathbf{u}(s',t)\cdot\mathbf{u}(s,0)\rangle$ is the probability density that, at time t, segment s' lies within the original tube at the place where s was initially. Integrating over s' gives us the probability $\Psi(s,t)$ that at time t *any* segment lies within the original tube at the place where segment s was initially. In other words, the chance that the original tube segment s is still up-to-date, is

$$\begin{aligned}\Psi(s,t) &= \frac{1}{d}\int_0^L \mathrm{d}s'\ \left\langle \mathbf{u}(s',t)\cdot\mathbf{u}(s,0)\right\rangle \\ &= \frac{4}{\pi}{\sum_{p=1}^{\infty}}'\frac{1}{p}\sin\left(\frac{p\pi s}{L}\right)\mathrm{e}^{-tp^2/\tau_d},\end{aligned} \tag{4.30}$$

where the prime at the summation sign indicates that only terms with odd p should occur in the sum. We have plotted this in Fig. 4.6. The fraction of the original tube that is still intact at time t, is therefore given by

$$\begin{aligned}\Psi(t) &= \frac{1}{L}\int_0^L \mathrm{d}s\,\Psi(s,t) \\ &= \frac{8}{\pi^2}{\sum_{p=1}^{\infty}}'\frac{1}{p^2}\mathrm{e}^{-tp^2/\tau_d}.\end{aligned} \tag{4.31}$$

This formula shows why τ_d is the time needed by the chain to reptate out if its tube; for $t>\tau_d$, $\Psi(t)$ is falling to zero quickly.

In conclusion we have found results that are in good agreement with Fig. 4.5. We see an initial drop proportional to $t^{-1/2}$; after that a plateau value G_N^0 independent of N; and finally a maximum relaxation time τ_d proportional to N^3.

Finally, we are able to calculate the viscosity of a concentrated polymer solution or melt of reptating chains. Using Eq. 2.70 we find

$$\begin{aligned}\eta &= \int_0^\infty \mathrm{d}\tau\, G(\tau) = G_N^0 \frac{8}{\pi^2} {\sum_{p=1}^{\infty}}' \frac{1}{p^2} \int_0^\infty \mathrm{d}\tau\, \mathrm{e}^{-\tau p^2/\tau_d} \\ &= G_N^0 \frac{8}{\pi^2} \tau_d {\sum_{p=1}^{\infty}}' \frac{1}{p^4} = \frac{\pi^2}{12} G_N^0 \tau_d. \end{aligned} \tag{4.32}$$

Since G_N^0 is independent of N, the viscosity, like τ_d, is proportional to N^3. This is close to the experimentally observed scaling $\eta \propto N^{3.4}$. The small discrepancy may be removed by introducing other relaxation modes in the tube model, which is beyond the scope of these lecture notes.

Problems

4-1. In Eq. (4.22) we have shown that, at short times, the shear relaxation modulus $G(t)$ decays as $t^{-\frac{1}{2}}$. We know, however, that $G(t)$ must be finite at $t = 0$. Explain how the stress relaxes at extremely short times. Draw this in Fig. 4.5.

4-2. In the tube model we have assumed that the primitive chain has a fixed contour length L. In reality, the contour length of a primitive chain can fluctuate in time. Calculations of a Rouse chain constrained in a straight tube of length L show that the average contour length fluctuation is given by

$$\Delta\bar{L} = \left\langle \Delta L^2 \right\rangle^{\frac{1}{2}} \approx \left(\frac{Nb^2}{3} \right)^{\frac{1}{2}}.$$

Show that the *relative* fluctuation of the contour length decreases with increasing chain length, i.e. that the fixed contour length assumption is justified for extremely long chains.

4-3. Can you guess what the effect of contour length fluctuations will be on the disentanglement times of entangled, but not extremely long, polymer chains? [Hint: See the first equality in Eq. (4.19)]. What will be the consequence for the viscosity of such polymer chains compared to the tube model prediction?

Index